UNIVERZA V LJUBLJANI
FAKULTETA ZA FARMACIJO

PIA REPŠE

MAGISTRSKA NALOGA
MAGISTRSKI ŠTUDIJ INDUSTRIJSKE FARMACIJE

Ljubljana, 2018

UNIVERZA V LJUBLJANI
FAKULTETA ZA FARMACIJO

PIA REPŠE

IZDELAVA IN VREDNOTENJE POLIKAPROLAKTONSKIH NANOVLAKEN S CIPROFLOKSACINOM IN METRONIDAZOLOM ZA PROTIBAKTERIJSKO DELOVANJE NA PARODONTALNE PATOGENE

PREPARATION AND CHARACTERISATION OF POLYCAPROLACTONE NANOFIBRES WITH CIPROFLOXACIN AND METRONIDAZOLE FOR ANTIBACTERIAL ACTIVITY ON PERIODONTAL PATHOGENS

MAGISTRSKI ŠTUDIJ INDUSTRIJSKE FARMACIJE

Ljubljana, 2018

Magistrska naloga je zaključek magistrskega študija industrijske farmacije na Fakulteti za farmacijo, Univerze v Ljubljani. Magistrsko nalogo sem opravljala na Fakulteti za farmacijo, Univerze v Ljubljani in na Erasmus+ izmenjavi na University of Tartu, Faculty of Medicine, Institute of Pharmacy pod mentorstvom prof. dr. Julijane Kristl in somentorstvom izr. prof. dr. Karin Kogermann. Uvodno srečanje z elektrostatskim sukanjem, slike z vrstičnim elektronskim mikroskopom, tekočinsko kromatografijo ultra visoke ločljivosti in pomoč pri pisanju mi je nudila mlada raziskovalka dr. Špela Zupančič v laboratoriju za farmacevtsko tehnologijo na Fakulteti za farmacijo, Univerze v Ljubljani in na Kemijskem inštitutu v Ljubljani. Meritve rentgenske difrakcije z uporabo X-žarkov je izvedel Jaan Aruväli na University of Tartu, Department of Geology.

Zahvala

Rada bi se zahvalila moji mentorici, prof. dr. Julijani Kristl za veliko predajo znanja, podpore in pomoči pri pisanju. Prof. dr. Karin Kogermann and Liis, I am extremely grateful that our paths crossed so I had the opportunity to learn from you. For all the kindness, advices and help in the institute, aitäh. Špela, hvala, ker si mi pomagala pri vseh korakih magistrske naloge, brez tebe mi ne bi uspelo. Nives, Nera, Tomi, Maša, Urška, Eva, Kaja, Maja in Barbara, hvala vam za vse skupne trenutke, moji študentski dnevi bodo zaradi vas nepozabni. Hvala mami in ati, da sta mi vedno stala ob strani, me spodbujala tekom celotnega študija in bila velika podpora za študijsko izmenjavo. Hvala tudi tebi stara mama za vse modrosti. Igor, saj veš.

Izjava

Izjavljam, da sem magistrsko nalogo izdelala samostojno pod mentorstvom prof. dr. Julijane Kristl in somentorstvom izr. prof. dr. Karin Kogermann. Naloga je bila izvedena v sklopu ARRS projekta J1-6746 pod vodstvom prof. dr. Julijane Kristl.

Pia Repše

Diplomska komisija

Predsednica: izr. prof. dr. Anamarija Zega

Mentorica: prof. dr. Julijana Kristl

Somentorica: izr. prof. dr. Karin Kogermann

Član: doc. dr. Jurij Trontelj

CONTENT

RAZŠIRJENI POVZETEK

Periodontitis je napredovano vnetje obzobnega tkiva, ki je sestavljen iz kosti zobiščnega odrastka, pozobnice, cementa in dlesni. Glavni vzrok za razvoj bolezni so parodontalni patogeni v kombinaciji s posameznikovim neustreznim imunskim odgovorom. Če periodontitisa ne zdravimo ustrezno, lahko vnetje napreduje do razgradnje kosti zobiščnega odrastka in izgube zoba. Pri tem tvegamo tudi razvoj drugih obolenj, kot so srčno-žilne bolezni, sladkorna bolezen in raznih zapletov v nosečnosti. Trenutno zdravljenje parodontalne bolezni temelji za mehanskem odstranjevanju zobnih oblog, nato pa parodontolog v primeru naprednih oblik bolezni zdravljenje nadaljuje z antibiotiki. Ker lahko sistemsko jemanje protimikrobnih zdravilnih učinkovin povzroči veliko neželenih učinkov, prav tako pa učinkovine težko dosežejo zobne žepe v zadostni koncentraciji, se razvoj zdravljenja periodontitisa usmerja v lokalno zdravljenje. Na tržišču so prisotna vlakna, trakovi in poltrdne farmacevtske oblike z vgrajenimi učinkovinami, vendar trenutne oblike predstavljajo neustrezno mehansko pritrditev in kasneje prehitro odstranitev za učinkovito delovanje oziroma nezadostno dostavljanje učinkovine na tarčna mesta v obzobnem tkivu. Za rešitev teh problemov so zelo obetavna nanovlakna z eno ali več zdravilnimi učinkovinami.

Cilj magistrske naloge je bil razvoj in izdelava čim tanjših, homogenih in netoksičnih nanovlaken z vgrajenimi protimikrobnimi učinkovinami s podaljšanim sproščanjem, ki bi uspešno delovala proti parodontalnim patogenom.

Nanovlakna smo izdelali z metodo elektrostatskega sukanja pod čimbolj enakimi procesnimi in okoljskimi pogoji. Prvi korak v izdelavi je izbira primernega polimera, ki je kompatibilen z želenimi učinkovinami in biokompatibilen s tkivi, s katerimi bo v stiku. Izbrali smo polikaprolakton (PCL), ki je netoksičen in odobren s strani agencije Združenih držav za hrano in zdravila (FDA) in Evropske agencije za zdravila (EMA). Nanovlakna smo pripravili iz 15% (m/m) polimerne raztopine pripravljene v ocetni in mravljični kislini v razmerju 3:1 (m/m). V nanovlakna smo vgradili 5% metronidazola (MTZ), ki je sintetična protimikrobna učinkovina in sodi med nitroimidazole ter deluje proti Gram pozitivnim in Gram negativnim bakterijam, kot tudi parazitom. Druga nanovlakna pa so vsebovala 5% ciprofloksacinijevega hidroklorida (CPR), ki spada v družino fluorokinolonskih protibakterijskih učinkovin in deluje proti Gram

negativnim bakterijam. Tretja nanovlakna pa so vsebovala po 2,5% tako MTZ, kot tudi CPR. Iz raztopine smo pod električno napetostjo z metodo elektrostatskega sukanja izdelali nanovlakna. Vpliv procesnih in okoljskih pogojev smo preverjali tako, da smo prva nanovlakna preverjali na objektnih stekelcih pod svetlobnih mikroskopom. Za izdelavo nanovlaken smo izbrali pogoje, pri katerih so bila nanovlakna brez vozlov, najtanjša in najbolj homogena. Izdelali smo tudi nanovlakna brez učinkovin. Morfologijo in premer nanovlaken smo ocenjevali s pomočjo SEM slik. Najtanjša nanovlakna so bila pri elektrostatskem sukanju polimerne raztopine z MTZ in sicer 412 ± 337 nm. Sledila so nanovlakna brez učinkovine, nanovlakna s CPR in na koncu nanovlakna s kombinacijo učinkovin s premeri 502 ± 302 nm, 650 ± 356 nm in 1274 ± 481 nm v enakem vrstnem redu. Slike, posnete z vrstičnim elektronskim mikroskopom (SEM), so tudi pokazale, da imajo nanovlakna s CPR in kombinacijo učinkovin veliko vozlov ter nanokristale na sami površini, ki bi lahko bila tudi sama nevgrajena učinkovina. Takšna nanovlakna niso primerna za nov dostavni sistem zato smo morali postopek elektrostatskega sukanja optimizirati.

Ker nas je zanimalo, ali se kristaliničnost učinkovin in polimera spremeni po elektrostatskem sukanju, kot tudi njihovo sproščanje in fizikalna stabilnost, smo izvedli meritve z diferenčno dinamično kalorimetrijo (DSC), rentgensko praškovno difrakcijo (XRD), in infrardečo spektroskopijo (FTIR). Omenjene metode nam dajejo vpogled tudi v možne interakcije med polimerom in učinkovino, ki se lahko zgodijo med elektrostatskim sukanjem. S pomočjo DSC metode smo določali talilno temperaturo nanovlaken, fizikalnih zmesi in samih učinkovin. Vsa nanovlakna, fizikalne zmesi kot tudi delci polimera, so imeli talilno temperaturo med 58,30 °C in 59,94 °C, kar predstavlja tališče PCL. Tališče MTZ je pri 163,19 °C. Pri CPR smo prvi vrh opazili pri 148,34 °C in je predstavljal izparevanje klorovodikove kisline (HCl) iz vzorca, saj je CPR v obliki ciprofloksacinijevega klorida monohidrata. Drugi vrh se je pojavil pri 315,17 °C in ponazarja tališče kot tudi temperaturo razgradnje. Omenjenih vrhov značilnih za MTZ in CPR nismo opazili pri fizikalnih zmeseh in nanovlaknih, zato ta metoda ni bila primerna za določanje kristaliničnosti učinkovin. Rezultati XRD so nakazali, da je prah PCL v polkristalinični obliki, medtem ko sta učinkovini MTZ in CPR v kristalinični obliki. Primerjali smo difraktograma polimernih delcev in nanovlaken brez učinkovin in opazili, da so vrhovi pri nanovlaknih na enakih mestih, le da so nižji in širši, kar pomeni, da elektrostatsko sukanje zniža stopnjo kristaliničnosti polimera. Zmesi polimera in učinkovin v enakem razmerju, kot so v

danih nanovlaknih, so izkazovale enake značilnice obeh komponent, le da so bili odzivi manj intenzivni zaradi nižjih vsebnosti. Vrhove značilne za MTZ smo našli pri difraktogramu nanovlaken z MTZ in zmesjo učinkovin, kar nakazuje, da smo MTZ vgradili v kristalinični obliki in le-ta ni spremenil oblike v amorfno. Vrhovi so bili prav tako nižji in širši v primerjavi s fizikalno zmesjo, kar lahko pomeni, da elektrostatsko sukanje zniža kristaliničnost MTZ. Vrhov značilnih za CPR nismo opazili pri nobenem difraktogramu. CPR smo verjetno vgradili v amorfni obliki, kar se lahko zgodi pri elektrostatskem sukanju, ko topilo izhlapeva iz curka, iz katerega nastajajo nanovlakna. Pri FTIR študijah smo med seboj primerjali nanovlakna in fizikalne zmesi v enakih razmerjih polimera in učinkovin. Ugotovili smo, da nanovlakna z MTZ izkazujejo vrhove pri enakih valovnih številih kot fizikalne zmesi, le da so ti nižji in manj intenzivni, kar vodi do zaključka, da je MTZ prisoten v nanovlaknih in ne reagira s polimerom med elektrostatskim sukanjem. Pri nanovlaknih s CPR smo prišli do enakega zaključka, le da smo opazili manjši premik enega vrha proti višjemu valovnemu številu v primerjavi s fizikalno zmesjo. Po prebiranju literature smo zaključili, da je premik vrha prisoten zaradi vodikovih vezi med CPR in polimerom. Vlakna s kombinacijo učinkovin imajo prav tako nižje in manj intenzivne vrhove v primerjavi s fizikalno zmesjo v enakem razmerju polimera in učinkovin.

Sproščanje učinkovin v medij, ki predstavlja zobni žep, smo preverjali s stresanjem nanovlaken v fosfatnem pufru in merili koncentracijo učinkovin s tekočinsko kromatografijo ultra visoke ločljivosti ob različnih časovnih točkah. Ugotovili smo, da nanovlakna ne izkazujejo podaljšanega sproščanja učinkovin, kot smo želeli. 72% MTZ se je iz nanovlaken sprostilo že v prve pol ure testiranja. Pri sproščanju CPR smo v prve pol ure prav tako opazili hitro sproščanje nad 35%. Če primerjamo sproščanje učinkovin iz vlaken, kjer smo vgradili kombinacijo obeh, se CPR sprosti primerljivo, MTZ pa v večji meri. Pričakovali smo podaljšano sproščanje, saj PCL kot izbrani polimer izkazuje hidrofobne lastnosti, ki zadržujejo difuzijo medija v notranjost nanovlaken, s katero bi se učinkovine lahko sprostile v obzobni žep. Vzroki za hitro sproščanje so lahko naslednji: učinkovina vgrajena na ali blizu površja nanovlaken; glede na učinkovino je bilo premalo PCL-ja, ki bi učinkovito zadržal difuzijo medija; nanovlakna so bila na določenih predelih poškodovana ali nehomogena.

Citotoksičnost nanovlaken smo preverili glede na standardne ISO predpise za testiranje citotoksičnosti materialov, ker nanotoksični standardi še niso opredeljeni. Sposobnost preživetja

fibroblastov smo testirali posredno in neposredno in jo opredelili kvalitativno in kvantitativno. Razlike v odstotkih preživelosti med neposredno in posredno metodo so statistično nepomembne. Kvalitativno smo opazovali morfologijo celic in njihovo pritrjenost na površino. Ocenili smo, da katerakoli testirana nanovlakna ne vplivajo na celično morfologijo ali pritrjenost na površino v primerjavi z negativno kontrolo. Kvantitativno smo s pomočjo avtomatskega števca živih in mrtvih celic izračunali celično sposobnost preživetja. Pri testiranju smo ugotovili, da je preživelost fibroblastov pri nanovlaknih brez učinkovine, z MTZ, CPR in s kombinacijo obeh nad 60%. Enak rezultat smo dobili tudi pri negativni kontroli, medtem ko smo pri pozitivni kontroli dobili število celic pod mejo detekcije. Zanimala nas je predvsem citotoksičnost PCL ter vzorcev in v primerjavi z ostalimi študijami lahko zaključimo, da so nanovlakna iz PCL varna za uporabo.

Učinkovitost nanovlaken smo preverjali z difuzijskim testom. Na gojišča smo nanesli parodontalne patogene, nato nanovlakna izrezana v obliki diska, pozitivne in negativne kontrole in opazovali spremembe v rasti po treh dneh gojenja bakterij v anaerobnih pogojih. Rezultate smo med seboj primerjali glede na premer inhibicijskega območja okoli diskov. Nanovlakna s CPR so bila učinkovita proti vsem testiranim bakterijam: *Porphyromonas gingivalis, Fusobacterium nucleatum, Aggregatibacter actinomycetemcomitans* in *Streptococcus mutans*. Premer inhibicijskih območji si sledi v enakem vrstnem redu, kar pomeni, da je CPR najbolj učinkovit proti *P. gingivalis*. Nanovlakna z MTZ so bila še bolj učinkovita proti *P. gingivalis* v primerjavi s CPR kot tudi proti A. *actinomycetemcomitans.* Delovala so tudi na *F. Nucleatum,* niso pa pokazala aktivnosti proti *S. mutans*. Zaključimo lahko, da so vlakna s kombinacijo MTZ in CPR optimalna izbira pri delovanju proti testiranim bakterijam, saj pokrijejo večji spekter protibakterijskega delovanja.

Ugotovili smo, da je optimizacija pogojev pri elektrostatskem sukanju ključna za izdelavo čim tanjših in homogenih nanovlaken. Glede na SEM slike, učinkovini MTZ in CPR ne vplivata na sam premer nanovlaken. S študijami DSC, XRD in FTIR smo ugotovili, da interakcij med polimerom in učinkovinami ni, potrdili pa smo tudi kristaliničnost vgrajenega MTZ po elektrostatskem sukanju. Pri opazovanju študij sproščanja učinkovin v medij, smo opazili, da nanovlakna ne izkazujejo podaljšanega sproščanja zaradi nehomogene oziroma poškodovane strukture ali vgrajenosti preblizu površja. Izdelana nanovlakna so po testiranih

ISO standardih netoksična. Učinkovitost proti izbranim paradontalnim patogenom je največja pri vlaknih s kombinacijo obeh učinkovin, kar smo preverili z meritvami inhibicijskih območij na agar ploščah.

KLJUČNE BESEDE: paradontalni patogeni • nanovlakna • metronidazol • ciprofloksacin • citotoksičnost

ABSTRACT

Periodontal disease is a severe inflammation of the periodontium, which leads to formation of the dental pockets, reduction of the alveolar bone and tooth loss. The main cause is the microbial shift with increased number of periodontal pathogens. Since current treatment lead to some side effects and reoccurrence of the disease, a new therapy is needed. One of the promising directions is a local treatment with new drug delivery systems, such as nanofibers.

In this study, we prepared different polycaprolactone (PCL) nanofibers using electrospinning without any drug, with incorporated 5% (w/w) of metronidazole (MTZ), 5% (w/w) ciprofloxacin (CPR) and a combination of both drugs with 2.5% (w/w) of each. Based on SEM images, the thinnest nanofibers were the one with MTZ with a diameter of 412 ± 337 nm, then nanofibers without any drug of 502 ± 302 nm and nanofibers with CPR of 650 ± 356 nm. The nanofibers with a combination of both drugs had the largest average diameter of 1274 ± 481 nm. XRD results showed that PCL possessed semi-crystalline structure while electrospinning slightly decreased its crystallinity. MTZ was incorporated into nanofibers in crystal form even though at lower level due to electrospinning. CPR was probably incorporated in an amorphous state, whereas nanocrystals were observed on the surface of nanofibers. FTIR studies showed that CPR and PCL according to FTIR shift interacted with each other forming hydrogen bonds. All drugs possessed burst release from nanofibers in the first half an hour. The safety of nanofibers was evaluated with standard ISO cytotoxicity tests on Baby hamster kidney fibroblasts by direct and indirect method. We concluded that PCL nanofibers with and without CPR and MTZ were safe because there was no statistically significant difference in viability comparing with pure PCL samples and the negative control. Disk diffusion assay was the method of choice for testing the efficacy of nanofibers against periodontal pathogens: *Fusobacterium nucelatum subsp. polymorphum*, *Streptococcus mutans*, *Aggregatibacter actinomycetemcomitans* and *Porphyromonas gingivalis*. Optimal choice against tested bacteria were a combination of fibers with CPR and MTZ.

To sum up, developed nanofibers with incorporated different antimicrobial agents immediately released the drug, were non-toxic on eukaryotic cells and effective against periodontal pathogens.

KEYWORDS: periodontal pathogens • nanofibers • metronidazole • ciprofloxacin • cytotoxicity

ABBREVIATIONS

API - active pharmaceutical ingredient

AUC - area under the curve

BHK - baby hamster kidney cells

CPR - ciprofloxacin HCl

DNA - deoxyribonucleic acid

DSC - differential scanning calorimetry

EDTA - ethylenediaminetetraacetic acid

EMA - European Medicines Agency

FDA - United States Food and Drug Administration

FTIR - Fourier-transform infrared spectroscopy

HCl - hydrochloride

HEPES - (4-(2-hydroxyethyl)-1-piperazineethanesulfonic acid)

ISO - International Organization for Standardization

LB - Lysogeny broth

MIC - Minimal inhibitory concentration

MTZ - metronidazole

PCL - polycaprolactone

SEM - scanning electron microscopy

UHPLC - ultra-high performance liquid chromatography

XRD - X-Ray Diffraction

1 INTRODUCTION

1.1 TEETH AND MICROBIOTA

The main function of human teeth is chewing and chopping food. It connects external environment with our inside through oral cavity. A part called periodontium (gr.: around the tooth) consists of alveolar bone (part of basal bone, where teeth are growing), periodontal ligament (tissue that connects the bone and the tooth), cementum (part of a tooth where ligaments are attached) and gingiva (gums) (Figure 1) (1).

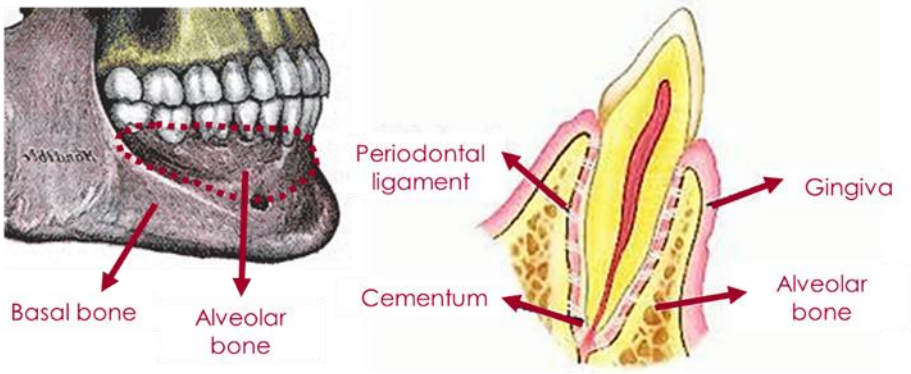

Figure 1: One the left is the picture of an alveolar bone and on the right a cross section of a tooth (adapted after reference 2).

The junction between teeth and gums has an important role in chewing. It enables the movement of our tooth when pressure is applied while eating. Nevertheless, this so called dentogingival junction has also an inconvenient feature due to moist environment and constant supply of nutrients. It is a perfect home for pathogen microbiota. When proper oral hygiene is not obtained, bacteria form a biofilm, which causes series of symptoms called periodontal diseases (1). The biofilm is a population of different microorganisms, which are adhered on different surfaces and protected by the polymeric substance produced by microorganism. It develops through four stages: free-floating, adhering, microcolonies and macrocolonies of microorganisms. The key factor for the growth of biofilm is communications between microorganisms. Once biofilm is formed, it is extremely difficult to completely remove it. The best treatment is the prevention of the pathogenic biofilm growth, where microbial shift occurs

and pathogenic bacteria overcome normal bacteria. However, there is also a positive role of dental biofilm: it provides mechanical and antimicrobial protection from outside environment and optimize the delivery of nutrients (3). Genetic and environmental factors also contribute to the development of this disease (1).

1.1.1 Development and causes of periodontitis

Healthy gums are pale pink (depending on ethnicity), firm and strong. The upper part of gums is free gingiva and it can be pulled away from the tooth so artificial dental pocket is created 1-3 mm in depth, and the lower gingiva is tightly attached. Gingival crevicular fluid flow through dental pocket is constant (a few μL per hour) and continuously delivers nutrients and washes away harmful substances. Immune response is mild due to normal microbiota (4, 5).Healthy gums and a development of periodontitis are presented in Figure 2.

Figure 2: Healthy gums and development of the periodontitis (adapted after reference 6).

Gingivitis means inflammation of gums, which are red, swollen, soft, mildly to severely painful, bleeding when irritated and warmer. The immune response is stronger than normal defense of healthy gums. The most common cause of this condition is the collapsed balance between beneficial and pathogenic microorganisms in dental pockets. It can also be caused by viral or fungal infections, genetic predispositions, allergic reactions, trauma and other factors (1). In this research, the focus will be on the plaque bacteria. The plaque is an adhesive film on

tooth, consisting of saline glycoproteins and antibodies, microorganisms and their extracellular polymer products, enzymes and inorganic components, such as calcium and phosphorus (7). If gingivitis remains untreated, it progresses, which can take some years, into disease called periodontitis or periodontal disease. Patients with weaker immune response develop periodontitis faster. When that happens, inflammation and immune response extend deep into connective tissue of teeth. Dental pockets become loose, gums move closer to alveolar bone and biofilm spreads to newly exposed tooth surface. The immune response becomes even stronger and symptoms get worse as long as the connective tissue loses attachment and the degradation of alveolar bone starts. When periodontitis worsen, the alveolar bone reduces which could lead to tooth loss. Periodontitis is a manifestation of systemic diseases and if it develops, there is a risk for cardiovascular diseases, diabetes mellitus and complications in pregnancy. On the other hand, cardiovascular diseases and some other causes, such as genetic changes, smoking and obesity are the reason for insufficient or excessive immune response. Therefore, periodontitis may be the cause or the consequence of other diseases (1, 8).

1.1.2 Periodontal pathogens

As mention before, dental plaque as biofilm is the main source of potential periodontal pathogens. It develops in relation of so-called dental pellicle (sin.: cuticula dentis, cuticula enameli, Nasmyth's membrane). This is an organic layer of specific proteins from saliva, which are selectively adsorbed on the tooth's enamel for protection of the tooth. First microcolonies are mostly Gram-positive bacteria, which bind to dental pellicle and to each other with hydrophobic and ionic bonds. These are streptococci (*S. sanguis, S. mutans, S. mitis, S. salivarius, S. oralis, S. gordonii*), lactobacilli and *Actinomyces*. Later macrocolonies are Gram-negative anaerobic bacteria (*Porphyromonas, Prevotella, Fusobacterium, Veillonella* species), anaerobic spirochetes and also *Actinomyces,* which bind to first colonies and with each other in the same way as first stages of dental plaque. In dental biofilm, there are 300-400 species of different bacteria. In Figure 3, relevant bacterial strains are presented in the formation of dental plaque (9).

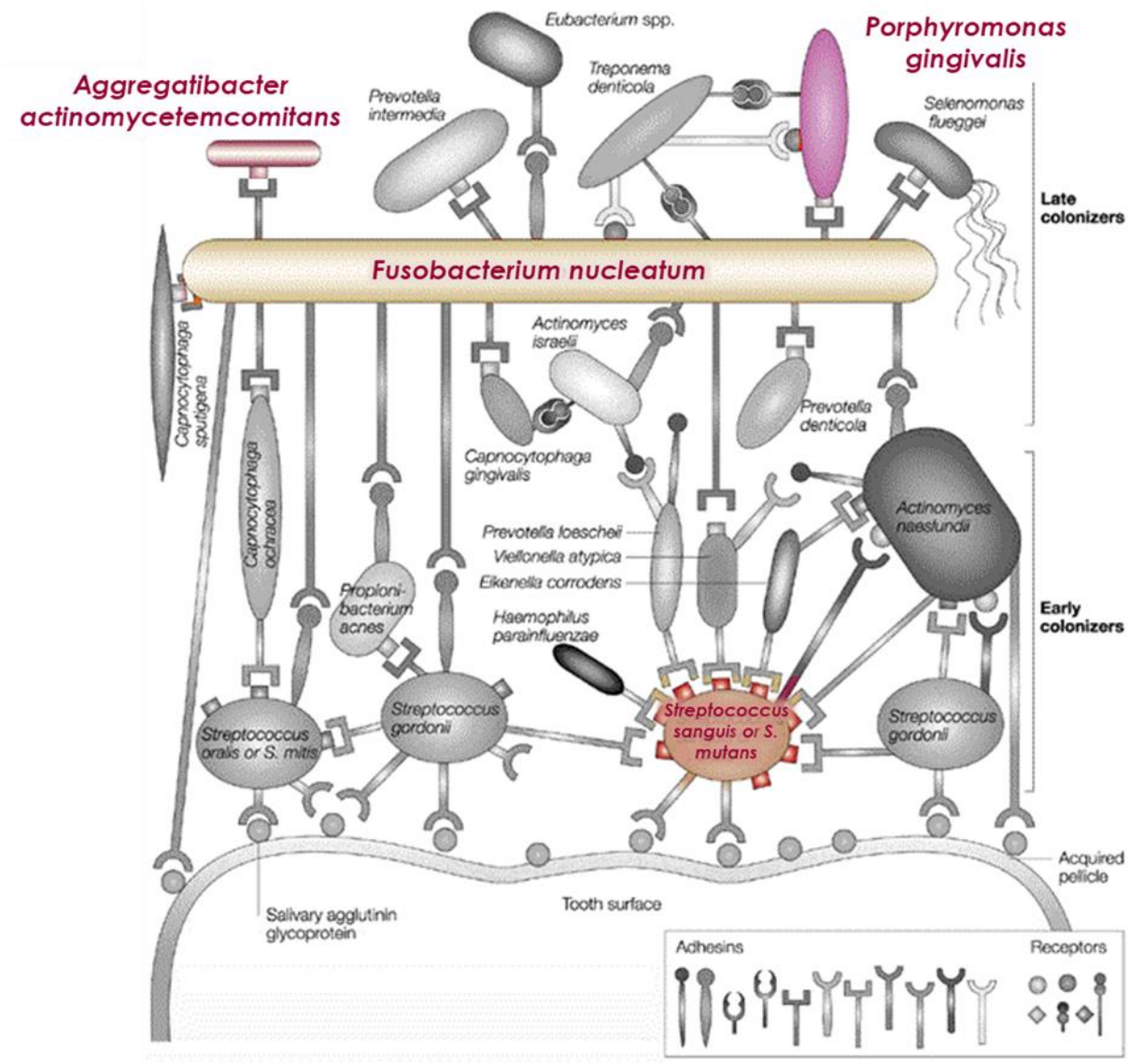

Figure 3: Early and late colonizers of the dental biofilm (adapted after reference 10).

1.1.3 Treatment of periodontitis

The best defense against the development of dental biofilm is prevention. Good oral hygiene and regular visits at the dentist are the key for oral health. If the infection of gums occurs, the first step is a mechanical removal of the dental plaque. Skills of the operator and the patient's maintenance of the proper hygiene after the procedure play an important role in suppression of the infection. The immune system of the patient is also an important factor in the healing and development of this disease. If the first step does not help, the doctor should set a

precise diagnosis. The depth of the dental pockets is in correlation with the severity of the periodontitis. The cause of periodontitis, which is sometimes hard to determine, are the main parameters to be taken into account. If there is any other systemic disease causing the periodontal disease, this should be firstly taken care of. The next step is a microbiological diagnosis in the inflammatory lesions. When bacteria are detected and identified, suitable systemic antibacterial drug is chosen. Due to the diverse composition of the dental biofilm, the combination of different drugs is desirable. The application of systemic antibiotic or chemotherapeutic should be only given after the mechanical removal of the biofilm, otherwise the drug itself is not efficient (1, 11). Systemic treatment has also disadvantages. The drug may not reach targeted tissue or the reached concentration is low which could lead to resistance of bacteria. Side effects can appear in many cases. Each individual has different microbiota in his mouth and development of periodontitis thus differs. There are patients with only one tooth with severe gum damage and patients who have every other tooth with inflamed dental pockets. That is the reason for the development of local delivery systems. Currently available medicines for local treatment are fibers, chips or semi-solid dosage forms with incorporated drug. Mechanical attachment and removal (if the form is not biodegradable) of these systems can take some time, which is not convenient for the patients. Contact between bacteria and the drug could be too short timewise and limited penetration in the dental pockets observed disadvantage. Surgery of damaged dental pockets is performed by periodontist in case of deep dental pockets. Alternatives in the treatment of periodontal disease are establishment of normal oral microbiota with probiotics, modulation of immune response and regeneration of damaged periodontium with new delivery systems (liposomes, nanofibers and polymeric nanoparticles). Patients with cured periodontium should take special care to maintain good oral heath that the disease does not reoccur (1, 8, 11, 12).

1.2 METRONIDAZOLE

Metronidazole (MTZ) is a synthetic antimicrobial drug and is classified as nitroimidazoles chemotherapeutic (Figure 4) (13).

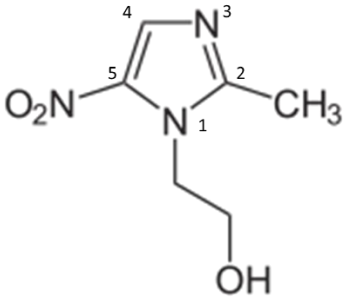

Figure 4: Chemical structure of metronidazole.

Pharmacodynamics: It is active against anaerobic Gram positive and Gram negative bacteria and against some parasitic infections. When it enters into bacterial cell, the reduction of nitro group (Figure 5) takes place. Results of this reduction are short-term living metabolites or free radicals with inhibitory or lethal effect on bacterial DNA (deoxyribonucleic acid) and other macromolecules. Nitroso radicals form adducts with DNA base pairs, which causes chain breaking of DNA and consequently bacterial cell's death. Cytotoxic metabolites later break into nontoxic and inactive secondary metabolites (13).

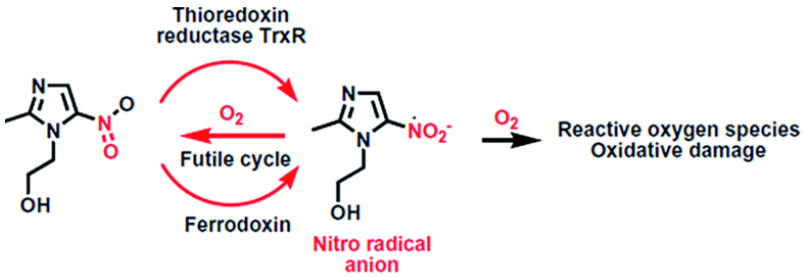

Figure 5: Formation of nitroso radical (nitro radical anion) (adapted after reference14).

Pharmacokinetics: Current application route of MTZ is oral, dermal and intravenous. Taken orally it absorbs quickly and almost entirely. Maximum serum concentration is similar in oral and intravenous use. Bioavailability is 90-100% and its half-life is 8 hours. MTZ has high volume of distribution, which reaches to 80% of body weight and it passes well into all

body's organs, tissues and body fluids. Plasma protein binding is up to 20%. The drug is metabolized in livers and eliminated with urine. 6-15% of dose is eliminated with faeces (13).

Indications and side effects: MTZ is indicated with bacterial infections of the central nervous system, lungs, gastrointestinal tract and abdomen, bones and joints and with gynecological and facial (including teeth) infections. MTZ is prescribed as prophylaxis before operations, where there is a big chance of anaerobic infections. Topical administration is used for acne rosacea treatment.

Side effects occur when MTZ is taken at high doses for longer periods. The most common are nausea, unusual taste in the mouth and risk of neuropathy. Common to rare side effects are headache, emesis, dizziness, high fever, dry mouth, superinfections with candida, diarrhea, severe hypersensitivity reactions, dark urine, hepatic impairment and others (13).

Chemical stability of metronidazole: MTZ is a white to pale crystalline powder soluble in water (1-10 g/100 mL at 20 °C, pH=5.8) (15). Because it is a weak base, it maximally dissolves at pH below 2. It is stable in open air and in aqueous solution at pH values from 1-8. Exposed to light, it changes its color to dark white to yellow, although in some studies it shows no degradation. pKa value for dissociation is 2.38 (16-19).

Metronidazole and periodontitis: MTZ is a commonly prescribed systemic medication for the treatment of periodontitis. It works against strictly anaerobic bacteria, which play an important role in the formation of dental biofilm. These bacteria are *Fusobacterium nucleatum*, *Porphyromonas gingivalis and Aggregatibacter actinomycetemcomitans* (in combination with other antibacterial drugs, for example ciprofloxacin) (11, 20-22). Minimal inhibitory concentration (MIC) for *P. gingivalis* treated with MTZ varies from 0.015-4 μg/mL (23, 24), for *F. nucleatum* MIC range is from 0.12–8 μg/mL (20, 24, 25) and for *A. Actinomycetemcomitans* from 0.38–256 μg/mL (26).

1.3 CIPROFLOXACIN HCl

Ciprofloxacin HCl (CPR) is a hydrochloride monohydrate salt of ciprofloxacin. It is an antibacterial drug, which belongs to a group of fluoroquinolones. In Figure 6, a chemical structure of CPR is presented (13, 27).

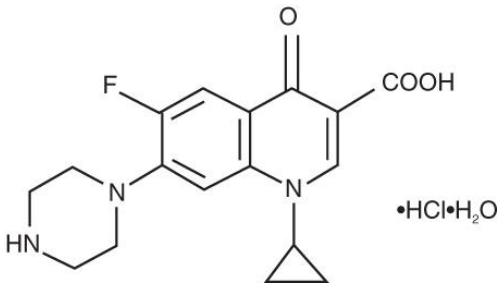

Figure 6: Chemical structure of ciprofloxacin HCl.

Pharmacodynamics: CPR inhibits bacterial isoenzymes topoisomerase II (DNA gyrase) and IV (Figure 7) by forming enzyme-DNA complex. Topoisomerases are enzymes that temporarily break and then reconnect phosphodiester bonds to unravel and unfold the double-strain DNA for replication or transcription. If that process is interrupted, bacterial cell cannot replicate which leads to cell's death (7, 28).

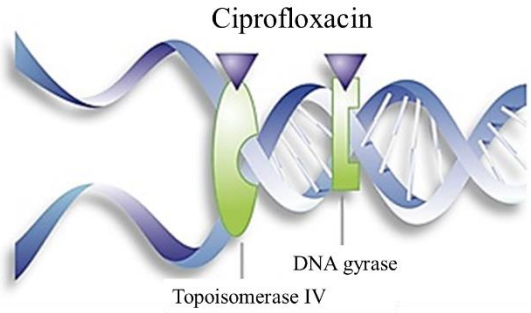

Figure 7: Mechanism of action of Ciprofloxacin HCl on bacterial DNA.

Pharmacokinetics: CPR is administrated orally, intravenously and intraocularly. Taken orally, CPR absorbs quickly and almost entirely. The maximum serum concentration is reached 1-2 hours after application. Serum concentration increases proportionally to 1000 mg. Bioavailability is 70-80% and plasma protein binding is 20-30%. CPR in plasma is predominantly in non-ionized form. The volume of distribution is high (2-3 L/kg per body

weight). High concentrations of a drug can be found in lungs, sinuses, urogenital tract and inflammatory lesions where total concentrations outreach plasma concentrations. Metabolism of CPR partially happens in liver and there are four known metabolites named oxociprofloxacin, desethyleneciprofloxacin, sulfociprofloxacin and formilciprofloxacin. The drug is mostly eliminated with urine in unchanged form and the rest by faeces. 1% is eliminated with bile. Its halt life is 4-7 hours. Pharmacokinetics by the intravenous administration is linear to dose of 400 mg. There is no difference in the area under the curve (AUC) in 60 min of 400 mg infusion and 400 mg tablet both in 12 hours or 60 min of 400 mg infusion in 8 hours and 750 mg tablet in 12 hours. When administrated intraocularly, it easily passes into the tissue. Systemic absorption is low (13).

Indications and side effects: CPR is indicated with bacterial infections of skin, soft tissues and lower respiratory tract with Gram negative bacteria, chronic purulent infections of the middle ear, chronic sinusitis, infections of urogenital and gastrointestinal tract, intraabdominal, bone and joint infections, malignant infection of the outer ear and as prophylaxis or treatment for patients with neutropenia. It is also prescribed as prophylaxis for invasive infections with *Neisseria meningitides*. For treatment of cystic fibrosis and lung anthrax with children, there is a need for special attention and great-skilled doctor for dose adjustment (13).

Most common side effects are nausea and diarrhea (oral and intravenous application). Among rare we can find fungal infections, colitis, eosinophilia and other blood and lymphatic diseases, allergic reactions, anorexia, hyperglycemia, psychiatric disorders, headache, dizziness, sleep, taste, sight and hearing disorders, tachycardia, dyspnea, vomiting, skin rashes, photosensitive reactions, renal impairment and others (13).

Chemical stability of ciprofloxacin: CPR is a pale yellow crystalline powder (29). It is highly soluble at pH below 5 and above 10. Because is it a zwitterion, it has its isoelectric point at 7.42, where it is also the least soluble. pK_1 value of substance is 6.17 and pK_2 is 8.54 (30, 31). It should be stored in tight, light resistant container at 25 °C, although stability studies showed, that even in acidic environment at 50 °C after 5 days there is no sign of degradation. Stored at 90 °C for 4 days, the degradation was around 4% (27, 30-32). There has been quite a

number of studies on interactions of fluoroquinolones with metal ions. If CPR is taken with medicine that contains multivalent cations and mineral excipients the bioavailability of CPR decreases. In addition, the increased concentration of metal ions enhances CPR degradation (13, 33).

Ciprofloxacin and periodontitis: Efficacy of CPR depends on the ratio between maximum serum concentration and MIC for certain bacteria (13). For the treatment of periodontal disease, CPR 500 mg tablets are taken twice a day for 8 days. Because of the variety of periodontal pathogens, it can be applied with combination of MTZ (11, 34). CPR is effective against *A. actinomycetemcomitans* with MIC 0.25-1 μg/mL, *P. gingivalis* with MIC 0.75-16 μg/mL and *F. nucleatum* with MIC 0.015–16 μg/mL (25, 28, 35-38). Scientists share different opinion about CPR antibacterial activity against *Streptococcus mutans*. Some say it is effective and some say *S. mutans* is resistant against that drug. (39-41). Johnston et al. showed MIC for CPR against *S. mutans* at 10 μg/mL and CPR incorporated in polymeric fibers with other combined drug at 1 μg/mL (42).

1.4 NANOFIBERS

Nanofibers are defined as very thin, solid fibers made of different polymers. The length of nanofibers can be theoretically infinite but the diameter of a single nanofiber is in nanometric scale. High ratio between surface and volume, porosity, flexibility and mechanical strength are some of the main qualities that nanofibers possess. As a consequence, they are used in many areas, such as textile industry, tissue engineering, cosmetics, electronic devices, filters and many more. Most common use in medicine and pharmacy are nanofibers as carriers for active pharmaceutical ingredient (API), maintaining homeostasis and nanofibers can be used as wound dressings (43-49). In Figure 8, there is a presentation of nanofibers in macro and micro scale.

Figure 8: PCL nanofibers on aluminum foil (left) and under scanning electronic microscope (right).

1.4.1 Preparation of nanofibers

There are several methods for nanofiber preparation: drawing, electrospinning, forcespinning, interfacial polymerization, melt blowing, phase separation, self-assembly, template melt extrusion and template synthesis (46, 49). Nanofibers are made from polymers, solvents for polymers and other excipients, such as surfactants and salts. Selection of a polymer is very important due to desired characteristics of nanofibers. The goal is a preparation of biocompatible, biodegradable, nontoxic, slightly hydrophilic, mechanically and thermally stable nanofibers. Polymers can be of natural or synthetic origin. Some natural polymers are chitosan, collagen, hyaluronic acid, elastin, alginate, cellulose; and some synthetic poly(vinyl alcohol) (PVA), poly(ethylene oxide), polycaprolactone (PCL), poly(glycolic acid) and poly(vinylpyrolidone). Polymers need to dissolve in the chosen solvent and not degrade in the

span of time needed for electrospinning process. The most commonly used solvents are acetone, dichloromethane, methanol, ethanol, acetic acid, ethyl acetate, formic acid and others (45, 46, 49).

1.4.1.1 Electrospinning

Most often used method for nanofiber preparation is electrospinning due to manipulation of fiber diameter, porosity (density of nanofiber layer) and fiber weight per area. However, there are also disadvantages of electrospinning: low process efficiency, cleaning of a nozzle and discontinuity of the process. Typical equipment for electrospinning is composed of a syringe with polymeric solution, a nozzle that is connected with high voltage supply, and a collector (Figure 9) (12, 49, 50).

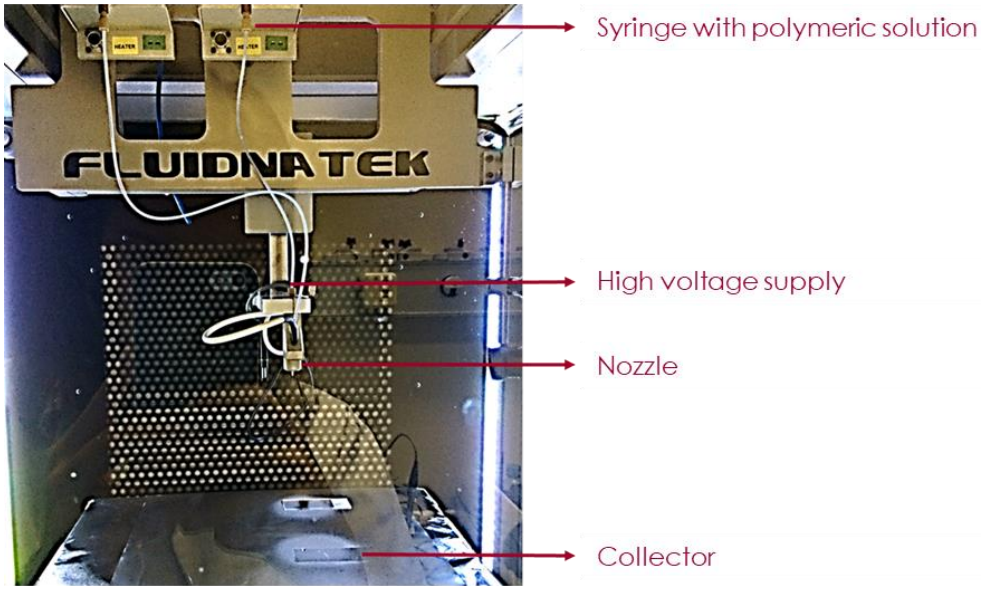

Figure 9: Equipment for electrospinning of nanofibers with marked basic components.

When polymer, API, excipients and their concentrations are chosen, they are dissolved in a suitable solvent. The solution is added into the syringe with a pump that creates a constant flow of liquid through tube to a nozzle. The nozzle is connected to high voltage supply, which causes a charged jet of polymeric solution. This jet can be in many forms depending on applied voltage and other parameters. Optimal shape of jet for nanofibers is cone-jet or Taylor's cone (Figure 10).

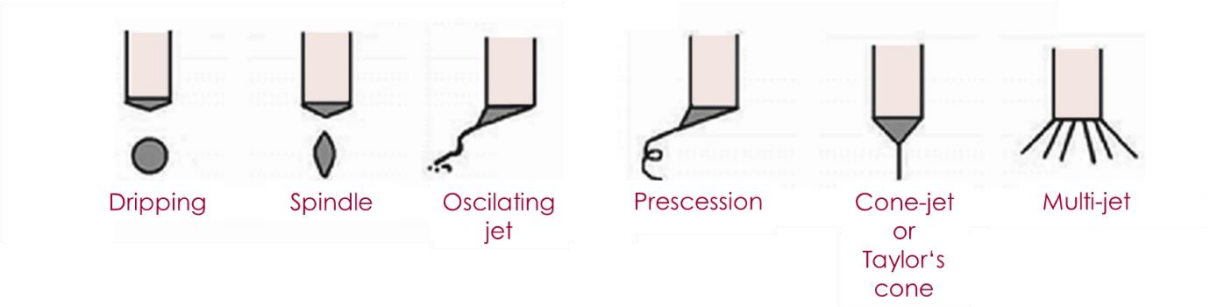

Figure 10: Many forms of the polymeric jet from nozzle under applied voltage (adapted after reference 51).

Jet is getting thinner as it is approaching to the collector, which allows solvents evaporation. Polymer becomes solid and it gathers on a collector. This thin layer of polymer deposit is called nanofibers (44, 51, 52). Parameters that are important in electrospinning process are solution, process and ambient parameters. They are presented in Table I (49).

Table I: Parameters in electrospinning process.

SOLUTION PARAMETERS	PROCESS PARAMETERS	AMBIENT PARAMETERS
- polymer characteristics (molecular weight, linearity, polyelectrolyte nature)	- applied voltage	- temperature
- polymer concentration	- distance from nozzle tip to collector	- relative humidity
- surface tension	- flow rate	
- rheological characteristics	- nozzle design	
- conductivity	- collector	
- dielectric constant		
- radius of gyration		

1.4.1.2 Example polymer for electrospinning - Polycaprolactone

Basic unit of this polymer is caprolactone. 'Capro' stands for caproic or hexanoic acid and 'lactone' is a name for cyclic ester of lactic acid. It is synthesized with ring-opening polymerization of ε-caprolactone (Figure 11) or with condensation of 6-hydroxycaproic acid.

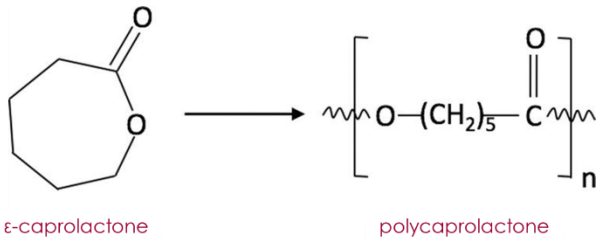

Figure 11: Chemical structure of ε-caprolactone and its polymerization in polycaprolactone (adapted after reference 53).

PCL is slowly biodegradable, biocompatible, non-toxic, semi-crystalline polymer. Its crystallinity can reach 69%, depending on the molecular weight and it determines the melting temperature, which is in the range of 56-65 °C and glass transition temperature from - 65 to -60 °C. Crystallinity is also important in the terms of permeability and biodegradability. Lower molecular weight results in higher crystallinity and lower permeability. PCL is soluble in organic solvents at room temperature (e.g. chloroform, benzene, toluene, cyclohexanone, acetone, ethyl acetate, acetonitrile, formic acid) and insoluble in alcohols, petroleum ether, diethyl ether and water (12, 54-56).

1.4.2 Nanofibers characterization

It is very important for the verification of nanofiber properties. Chemical and mechanical properties, morphology and nanofiber thermal behavior can be observed with different methods. Optical microscopy is used for the easier optimization of electrospinning process, while nanofibers morphology specifically is investigated by scanning electron microscopy (SEM). Crystallinity is characterized with X-ray diffraction (XRD) and differential scanning calorimetry (DSC). Infrared spectroscopy (IR) is used for determination of any structural changes of the polymer and interaction between the polymer and the drug that may occur during electrospinning. There exist many other techniques for characterization of nanofibers (49, 50).

1.4.3 Nanofibers and periodontitis

The nanofibers used as new local drug delivery system for treatment of periodontal disease should deliver the drug into the base of the dental pocket with concentration above MIC and provide prolonged release to be clinically effective. The placement should be simple, noninvasive, painless and durable. So far, there are fibers on the market that are replaced every week, which leads to bad patient compliance. The selection of polymer with slow degradation and controlled release of a drug is a solution. PCL poses this characteristic due to its semi-crystalline and hydrophobic nature; is non-toxic and highly permeable to many drugs. When periodontitis is treated locally, dose of antimicrobial agent will be much lower although higher at targeted place than treated systemically, which can reduce the occurrence of side effects. The local administration can also avoid the first pass metabolism and other gastrointestinal issues. Ideally, targeting of a drug should be only against periodontal pathogens and not against normal microbiota. This activity is hard to achieve, but with finding the differences between the susceptibility of periodontal and normal bacteria to API can be beneficial. Due to similarity of structure and function between nanofibers and extracellular matrix, nanofibers have great biomimetic characteristics. They provide good adhering area for the cells and they are porous enough to exchange nutrients and metabolites (12, 46, 48, 57-61). In Figure 12, the local application of nanofibers into periodontal pocket is presented.

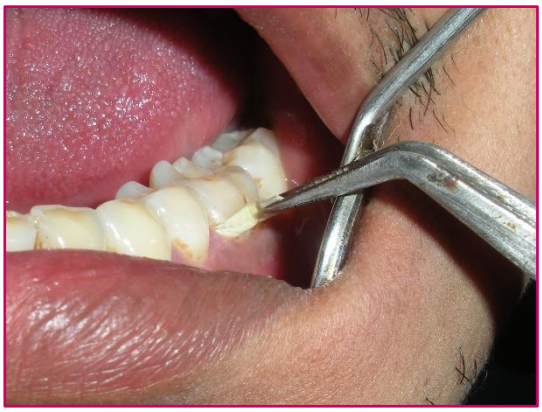

Figure 12: Application of nanofibers in the dental pocket (adapted after reference 62).

2 RESEARCH OBJECTIVES

Specific targeting of API into dental pocket represents a challenge in the development of local treatment of periodontal disease. Nanofibers present a promising option for patient-friendly delivery system with incorporated active ingredients. The purpose of this master thesis was to prepare non-toxic nanofibers with prolonged release of antimicrobial agents into the periodontal pockets specifically targeting oral pathogens. The following specific tasks were set:

- To **prepare uniform nanofibers without beads** using **electrospinning** at controlled process and ambient conditions. Selected polymer was PCL due to its biocompatibility, slow biodegradation, nontoxicity and easy handling. Incorporated antibacterial drugs were MTZ and CPR alone and in combinations to possibly achieve additive or synergetic effect against periodontal pathogens. **Homogeneity and diameter** of nanofibers was evaluated with SEM.
- Crystallinity of a PCL and incorporated drugs in nanofibers were verified with DSC and XRD method. For the comparison, physical mixtures of formulations were tested. Fourier - transform infrared spectroscopy (FTIR) was used for determination of structural changes of ingredients during electrospinning and possible occurrence of interactions between PCL and incorporated drugs.
- **Release of the drug** into small volume of phosphate buffer in glass vial, which illustrates gingival fluid, was determined with ultra-high performance liquid chromatography (UHPLC) method.
- **Safety** of nanofibers was evaluated by cytotoxicity tests on baby hamster kidney (BHK) fibroblasts in cell culture with direct and indirect method according to International Organization for Standardization (ISO) guidelines.
- **Antibacterial activity** of nanofibers against periodontal pathogens was verified with disk diffusion test on agar plates on relevant periodontal pathogens such as *Fusobacterium nucelatum subsp. polymorphum, S. mutans, A. actinomycetemcomitans* and *P. gingivalis* which all play important role in the formation of dental biofilm.

3 MATERIALS AND METHODS

3.1 MATERIALS

- Acetic acid, 100% (J. T. Baker, Germany) as solvent for PCL
- Baby hamster kidney fibroblasts BHK21
- Bacterial strains: *Escherichia coli* DSM 1103, *Fusobacterium nucelatum subsp. polymorphum* DSM 20482, *Streptococcus mutans* DSM 20523, *Aggregatibacter actinomycetemcomitans* DSM 11123, *Porphyromonas gingivalis* DSM 20709 (Leibniz-Institut DSMZ-Deutsche Sammlung von Mikroorganismen und Zellkulturen GmbH, Germany)
- Ciprofloxacin HCl monohydrate, (Alfa Aesar, Germany) as API
- Columbia agar base supplemented with 5% defibrinated sheep blood: nutrient Lennox lysogeny broth (LB) (Difco Laboratories, USA), Yeast extract Tryptone Medium (Difco, USA), Bacto Agar (BD, USA), L-Cysteine-HCl monohydrate (AppliChem, Germany), glucose, NaCl, defibirnated sheep blood (bioTRADING, The Netherlands) and commercial LabM, UK
- Formic acid, 98-100% (J. T. Baker, Germany) as solvent for PCL
- Glasgow Minimal Essential Medium (GMEM) supplemented with 7.5% FBS (Sterile 1x Phosphate buffer saline), 20 mM HEPES, 2% TPB (Tryptose Phosphate Broth), 100 units/mL Penicillin, 100 g/mL Streptomycin (Sigma Aldrich, USA)
- Liquid nitrogen for PCL powder (AGA, Estonia)
- Methanol, 10% and Acetonitrile, 98% (Merck, USA) as UHPLC mobile phases
- Metronidazole (Sigma Aldrich, USA) as API
- Oxygen absorbing bag, 2,5 L Anaerogen™ (Thermo Fisher Scientific Inc., USA)
- Polycaprolactone M_w=80 kDa (Sigma Aldrich, USA) as a carrier polymer
- Potassium dihydrogen phosphate and Sodium hydroxide (Merck, USA) for phosphate buffer as a release medium
- Triton X, 10% (BioTop, Austria) as a positive control in cytotoxicity testing
- Trypan blue, 0.4% (Invitrogen, USA) as a coloring agent for BHK
- Trypsin-EDTA, 0.05%-0.022% (Smart Media) as a detachment agent

All the chemicals were used as received without any further purification or modification.

3.2 LABORATORY EQUIPMENT

- Chromatographic system Acquity UHPLC (Waters Corp., USA) and Column with pre-column Acquity UHPLC (Waters Corp., USA)
- Countess™ Automated cell counter (Invitrogen, USA)
- DSC 4000 (PerkinElmer, USA) and Intracooler SP (PerkinElmer, USA)
- Electrospinning equipment Slovenia: Fluidnatek LE100; BioInicia SL, Spain
- Melt electrospinning (NanoNC Co., Ltd., Korea)
- Image J program (National Institute of Mental Health, Maryland, USA)
- Incubator, 37 °C, 5% CO_2 (Thermo Scientific Heraeus, UK)
- IR Prestige 21 (Shimadzu Corporation, Japan)
- Optical microscope
- Orbital rotator (Vibromix 403EVT, Slovenia)
- OriginLab program (Massachusetts, USA)
- SEM (high-resolution scanning electron microscope; Zeiss EVO® 15 MA, Germany)
- X-ray diffractometer (D8 Advance, Bruker AXS GmbH, Germany)

3.3 PREPARATION OF NANOFIBERS

3.3.1 Solution preparation

A solvent mixture of acetic and formic acid with the ratio of 3:1 (w/w) was used for the preparation of all 15% (w/w) PCL polymeric solutions unless otherwise stated. Polymer solution was prepared approximately 3 hours before electrospinning or the night before, in which case it was left in the refrigerator. Half an hour before electrospinning active ingredient was added, 5% (w/w) of MTZ, CPR or the mixture of both with the same concentration of 2.5% (w/w). The polymer solutions were used for electrospinning when all the components were fully dissolved in covered flask on the magnetic stirrer.

3.3.2 Electrospinning

The electrospinning conditions were optimized for each solution separately to obtain uniform, continuous and beadless nanofibers. Nanofibers were electrospun at flow 0.6 mL/h and voltage was in the 16-17 kV range. The inter-electrode distance was 15 cm. All nanofibers mats were collected on an aluminum foil on a flat surface.

3.4 NANOFIBERS MORPHOLOGY

The images of nanofibers were taken using SEM technique, operated at an acceleration voltage of 1 kV with a secondary detector. Diameters of 100 randomly selected nanofibers were measured with Image J program. Average diameter and standard deviation were calculated with MS Office Excel 2013.

3.5 PHYSICAL CHARACTERIZATION OF NANOFIBERS

3.5.1 Preparation of physical mixtures

In order to get comparable results, physical mixtures of PCL powder and drugs were prepared. PCL powder was made with crushing of melt electrospun PCL microfibers (prepared at 200 °C, a relative humidity (RH) of 16%, a voltage of 4 kV, a roller speed of 30 rpm, a flow rate of 2 mL/h) with liquid nitrogen in a mortar. Powder was unified with a sieve. Amount of MTZ, CPR and combination of these drugs in powder mixture was the same as in PCL nanofibers: 5% (w/w) of MTZ, CPR or the mixture of both with the same concentration of 2.5% (w/w).

3.5.2 Differential scanning calorimetry

The thermal analysis was performed using DSC of the next samples: PCL nanofibers with MTZ, CPR and with combination of both drugs. The results were compared with PCL nanofibers, powders of pure substances and powder mixtures. We weighed 1.6-3.6 mg of each sample into aluminum pans, covered with aluminum lid and made a pin hole in the middle of the lid. Pan and cover were pressed together with a pressing machine. The same DSC program was used for all the samples: hold for 3 min at 0 °C; heat from 0 °C to 190 °C at 10 °C/min;

hold for 1 min at 190 °C; cool from 190 °C to 0 °C at 10 °C/min. CPR powder was the only sample which required different DSC program: heat from 0 °C to 400 °C at 10 °C/min; hold for 1 min at 400 °C; cool from 400 °C to 0 °C at 10 °C/min. Since CPR started to degrade above 300 °C and the vapors could harm the machine, program was stopped at 338 °C. Nitrogen gas flow was 19.8 mL/min at 4.0 bar. Indium was used for the calibration of the equipment.

3.5.3 X-Ray Diffraction

XRD experiments were carried out in a symmetrical reflection mode (Bragg–Brentano geometry) with CuKa radiation (1.54 Å). The scattered intensities were measured with the LynxEye one-dimensional detector including 165 channels. The angular range was from 5° to 40° 2-theta with the step size of 0.0195° 2-theta. Analyzed samples were: PCL nanofibers, PCL nanofibers with MTZ, CPR and combination of the drugs; PCL, MTZ and CPR powder; physical mixtures of PCL and MTZ, PCL and CPR, PCL and combination of both drugs.

3.5.4 Fourier transformed infrared spectroscopy

FTIR measurements were carried out at the resolution of 4.0 cm^{-1} with an average of 60 scans in the spectral range from 600 to 4000 cm^{-1}. Normalisation was used as pre-treatment. The following samples were analyzed: PCL nanofibers, PCL nanofibers with MTZ, CPR and combination of both drugs; PCL, MTZ and CPR powder; physical mixtures of PCL powder with MTZ, CPR and combinations of both drugs.

3.6 DRUG RELEASE EXPERIMENTS

All nanofibers mats were cut into rectangular pieces weighing 12.0 ± 0.5 mg and put into a glass vial containing 20 mL of 50 mM phosphate buffer with pH 7.4 and covered with plastic cap. The vials with nanofibers were shaken with 150 rpm on an orbital rotator at room temperature. At pre-determined time intervals, 1 mL or release medium was withdrawn and replenished with a fresh buffer. 1 mL samples were diluted with 1 mL of phosphate buffer with pH 7.4. The samples were then filtered with 0.2 μm filter into small UHPLC vials to determine the quantity of released drug. There were three replicates performed.

3.6.1 UHPLC analysis

The UHPLC method was developed to separate and quantify MTZ and CPR. A UV–VIS photodiode array (PDA) module equipped with a high-sensitivity flow cell was used for detection. The column with pre-column was Acquity UHPLC CSH C18 1.7 μm 2.1 × 50 mm. A gradient elution was used to achieve chromatographic separation with mobile phases A (25 mM phosphate buffer with pH 3 and 10% methanol) and B (acetonitrile, containing 2% water). The mobile phase in the gradient elution progress was: 0–1 min 0% B, 3 min 20% B, 3.2-3.6 min 50% B, and 4.4-5.0 0% B. The flow rate was set at 0.5 mL/min, the column temperature was maintained at 50 °C, and the injection volume was 5 μL. The analytical run time for each sample was 5 min. Initial standard stock solutions of MTZ or CPR with concentrations of 1 mg/mL were further diluted with phosphate buffer with pH 7.4 in order to obtain seven standard solutions in the range of 0.5–40 μg/mL. Area under peak was used for calculation of drug concentration. The detector wavelength was set at 271 nm.

3.7 CYTOTOXICITY OF NANOFIBERS

Safety of the nanofibers was evaluated using a cytotoxicity test on BHK. Fibroblasts grew in the media we prepared ourselves: GMEM supplemented with FBS, 20 mM HEPES, 2% TPB, 100 units/mL Penicillin, 100 g/mL Streptomycin. Fibroblasts were checked under the optical microscope to see if they were attached on the bottom of the well and formed a near confluent monolayer in order to proceed with the experiment. Cytotoxicity method was performed in two different ways: direct and indirect. Cytotoxicity testing was performed according to the ISO guidelines (ISO 10993-5) (63).

3.7.1 Direct method

PCL nanofibers, PCL nanofibers with CPR, MTZ and with combination of the drugs (S=1 cm^2, 5 series) were each added to the near confluent fibroblasts in 1 mL of medium. Nanofibers were remained on the surface of the media. After 24 h in the incubator (37 °C, 5% CO_2), the cells were detached with trypsin and colored with trypan blue (10 μL of cell dispersion and 10 μL of trypan blue). Non-viable cells were colored blue, viable cells stayed unstained. Automated cell counter counted dead and live cells and calculated cell viability. Untreated cells

were used as a negative control and cells treated with 100 µL of Triton X acted as a positive control.

3.7.2 Indirect method

PCL nanofibers, PCL nanofibers with MTZ, CPR and with combination of the drugs (m=5 mg) were each put in 6 mL of medium. Fibroblasts were grown to near confluency on 24-well plate in the incubator (37 °C, 5% CO_2), then the media were replaced with media from nanofibers. Cells were incubated again for 24 h (37 °C, 5% CO_2) and then colored with trypan blue (10 µL of cell dispersion and 10 µL of trypan blue). Viability was checked as mentioned previously. Negative and positive controls were also the same. Comparison of both methods is presented in Figure 13. Statistical significance for methods of cytotoxicity was calculated with t-test with Origin PRO 2017 program. $P < 0.05$ was considered as the significant level.

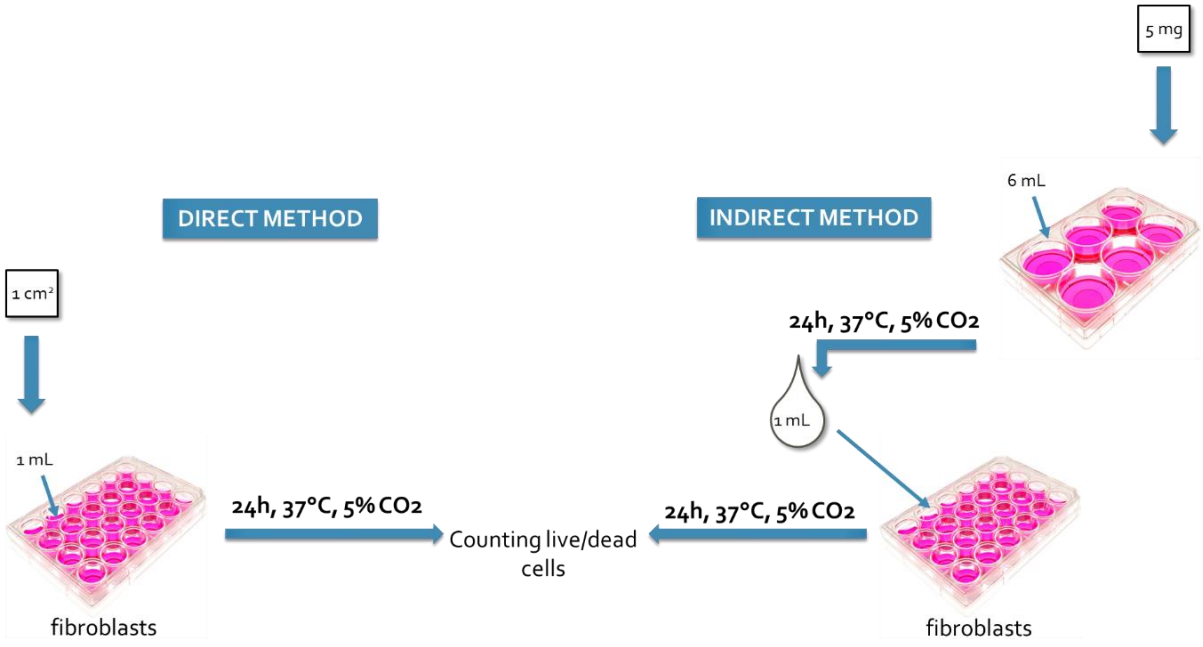

Figure 13: Comparison of direct and indirect method.

3.8 DISK DIFFUSION ASSAY OF NANOFIBERS ANTIBACTERIAL EFFICACY

Nanofibers antibacterial efficacy against aerobic and anaerobic bacteria was evaluated by using a disk diffusion assay and measuring the diameter of inhibition zones free from bacterial growth around the fiber disk. PCL nanofibers, PCL nanofibers with MTZ, CPR and combination of both drugs were cut as disks (d=6 mm) with punching machine. Negative control was UV-sterilized filter paper cut in the same way as nanofibers. Positive control was UV-sterilized filter paper soaked into 20 µL solution of MTZ, CPR or combination of the drugs in distilled water. Concentrations of these solutions were chosen to obtain the same calculated theoretical amount as within the nanofiber disks (1.5 mg/mL). Nanofibers efficacy was tested against the following relevant bacteria: *E. coli* DSM 1103, *F. nucelatum Subsp. Polymorphum* DSM 20482, *S. mutans* DSM 20523, *A. actinomycetemcomitans* DSM 11123 and *P. gingivalis* DSM 20709. *E. coli* was cultivated in aerobic conditions on plates made with this formulation: 8 g nutrient broth, 5 g yeast extract, 5 g NaCl, 2 g glucose, 16 g agar, dissolved in 1 L of water pH 7.0, autoclaving 0.5 atm. Overnight bacterial culture was first diluted in LB to obtain optical density of about 0.05 and then 100 µL of this dilution was spread over each plate and the prepared disks were put on top of it, incubated for 24 h at 37 °C. All other bacteria including *E. coli* were tested in anaerobic conditions. Bacteria grew on Columbia agar base supplemented with 5% defibrinated sheep blood. After bacteria were spread all over the plate, disks were put on top of them. Plates were then placed in a plastic bag with added oxygen absorbing bag, which was then hermetically sealed. Inhibition zones were checked after 3 days (incubated at 37 °C) due to slower growth of anaerobic bacteria. Tests were run in triplicate for each bacterium. Figure 14 presents the typical disk assay.

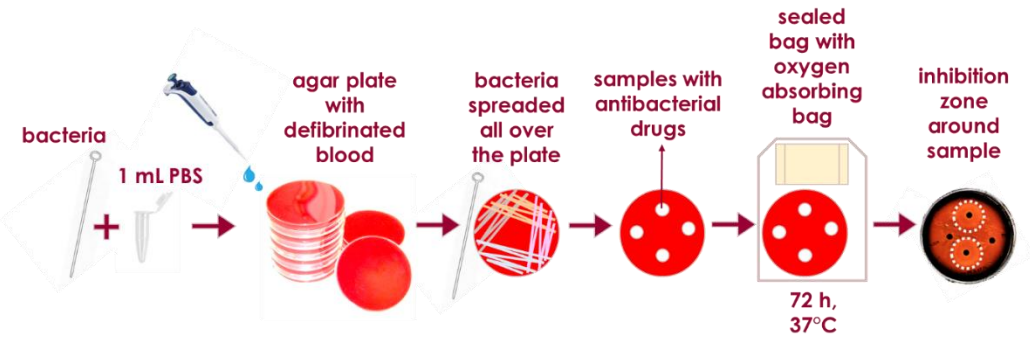

Figure 14: Disk diffusion assay performed on *Streptococcus Mutans* in aerobic conditions.

4 RESULTS AND DISCUSSION

4.1 NANOFIBERS MORPHOLOGY

The nanofibers morphology plays a key role in the mechanical properties and clinical efficacy, such as controlled drug release, and can be modified with the selected polymer solution, ambient and electrospinning parameters (64). To obtain the thinnest, straightest and most homogeneous fibers for optimal delivery system, we optimized electrospinning process via changing the applied voltage. The optimal applied voltage was chosen according to the shape and stability of Taylor cone. The first screening on the nanofibers morphology was performed with optical microscope and the most optimal nanofibers were analyzed in detail using SEM.

PCL nanofibers with incorporated 5% of MTZ, CPR and combination of both drugs with 2.5% of each were electrospun and compared with PCL nanofibers without drug. As seen in Figure 15A, PCL nanofibers without drug were uniform, continuous and with an average diameter of 502±302 nm. The incorporation of MTZ into nanofibers did not affect the nanofibers morphology, there were no crystals observed on the nanofibers surface and the average nanofibers diameter (412±337 nm) was slightly decreased, which is in line with the literature data (Figure 15B) (60, 65, 66). By contrast, the incorporation of CPR significantly affected the nanofibers morphology as it is seen from nanofibers with CPR and combination of both drugs (Figure 15C and D). Average diameter of nanofibers with CPR and combination of both drugs is 650±365 nm and 1274±481 nm, respectively. When average diameter of nanofibers outreaches the nanometer scale, they are no longer nanofibers but microfibers. In this study, fibers with combination of both drugs will be still called as nanofibers to ease the discussion. Some deposits that may be nanocrystals of CPR were observed on the nanofibers surface. According to the literature, addition of the CPR should not affect PCL nanofibers morphology (65-67). These non-homogenous nanofibers are not representative for a new prolonged drug delivery system for the treatment of periodontitis, but it is believed that the optimization of drug concentration within the fibers enables to avoid drug recrystallization on the fiber surface.

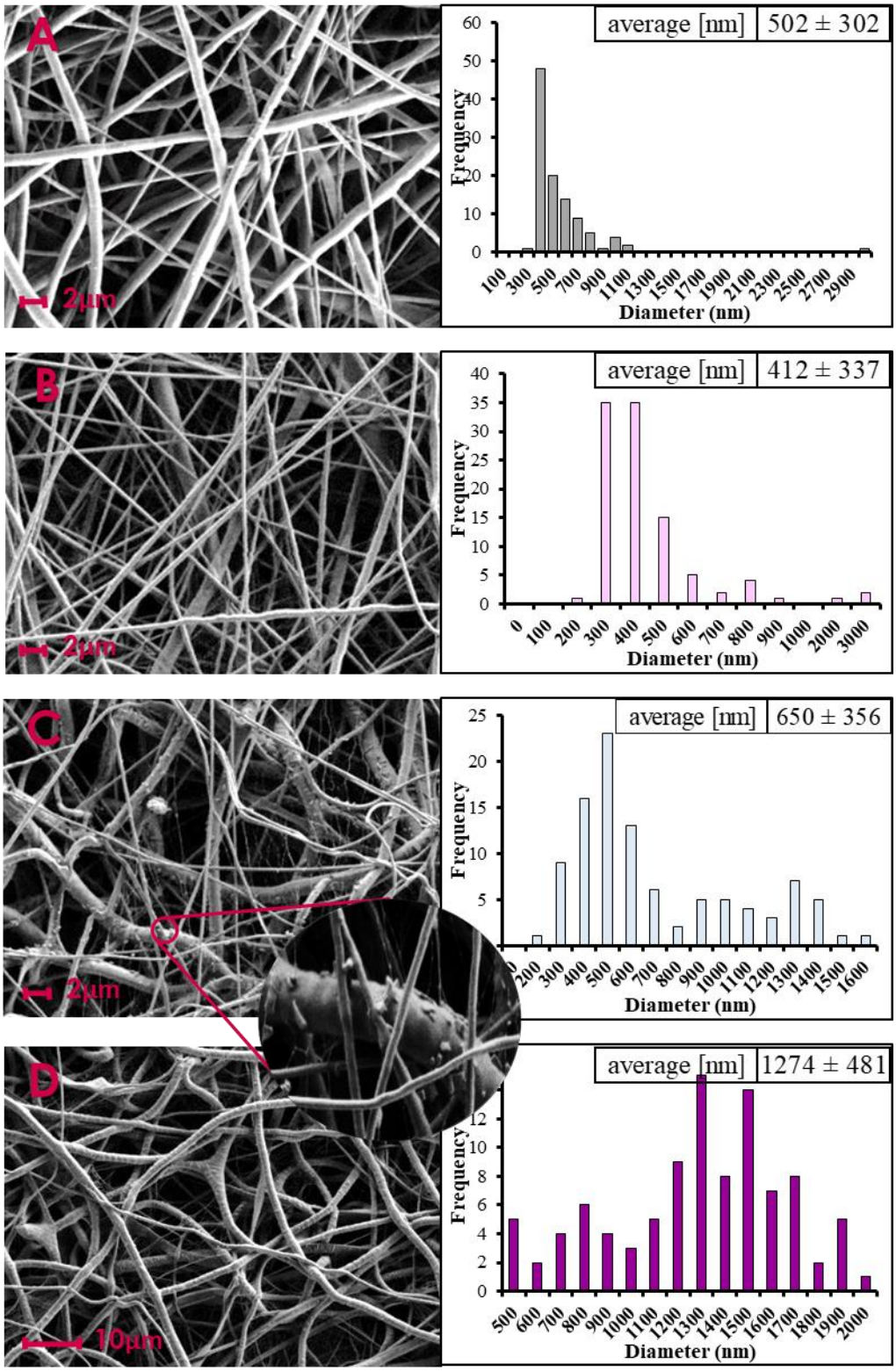

Figure 15: SEM images and histograms of size distribution of A) PCL nanofibers without any drug, B) metronidazole nanofibers, C) ciprofloxacin nanofibers and D) nanofibers with combination of both drugs.

4.2 PHYSICAL SOLID STATE CHARACTERIZATION OF NANOFIBERS

It was of interest to find out the solid state form of drugs within the nanofibers after electrospinning in order to obtained knowledge about their effect on dissolution behavior as well as physical stability. It is known that usually amorphous form of drug is obtained during electrospinning, since during quick evaporation of solvent, drug molecules do not have enough time to crystallize and polymer matrix stabilizes the amorphous form. FTIR additionally allows understading the intermolecular interactions between the drug and polymer as well as verify the solid state form of drug (68, 69).

4.2.1 Thermal analysis of nanofibers by DSC

DSC analysis was performed to determine melting temperature of blank PCL nanofibers and PCL nanofibers with MTZ, CPR and combination of both drugs. Furthermore, the crystallinity of the drugs and the polymer and possible changed properties as the consequence of electrospinning process were determined. Endothermic peaks in all cases except CPR powder represent melting temperature (Tm) of each sample. The melting temperature of PCL is between 58.30 °C and 59.94 °C observed in case of all nanofibers and physical mixtures (Figure 16a, d-i) and is in line with the literature (70). Melting point of MTZ was 163.19 °C (Figure 16b), which also correlates with the literature (71, 72). The peak of MTZ melting temperature was not present in physical mixtures and nanofibers with MTZ due to low quantity of a dispersed drug in physical mixture and nanofibers or the dissolution of MTZ in a melted polymer during heating (Figure 16d, e) (70, 73). CPR thermogram in Figure 17 shows two endothermic peaks. First endothermic peak occurs at 148.34°C (Figure 16c, Figure 17) and represents the evaporation of hydrate water from the sample, since the drug is hydrochloride monohydrate salt of ciprofloxacin. Second endothermic peak is at 315.17 °C and represents melting and degradation temperature of the drug (71, 74). Again, there was no endothermic melting peak in the samples representing physical mixtures and nanofibers with CPR since DSC measurements were not performed using temperatures above 300 °C (Figure 16f, g). Therefore, the crystallinity forms of the drugs in nanofibers could not be determined using DSC and XRD method was used for further analysis.

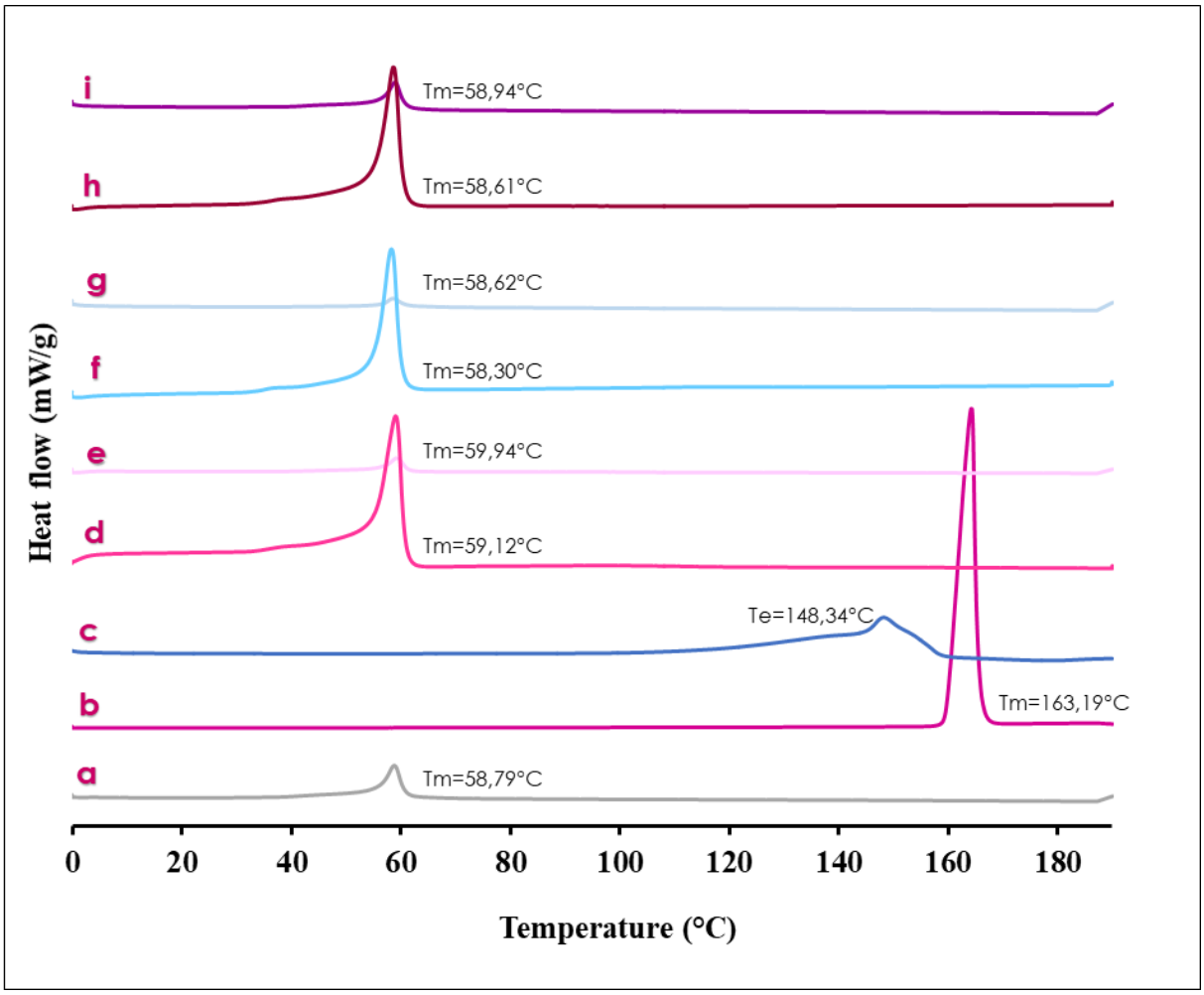

Figure 16: DSC thermograms of a) PCL nanofibers , b) metronidazole powder, c) ciprofloxacin powder, d) physical mixture of PCL + metronidazole, e) metronidazole nanofibers, f) physical mixture of PCL + ciprofloxacin, g) ciprofloxacin nanofibers, h) physical mixture of PCL and combination of both drugs and i) PCL nanofibers with combination of both drugs.

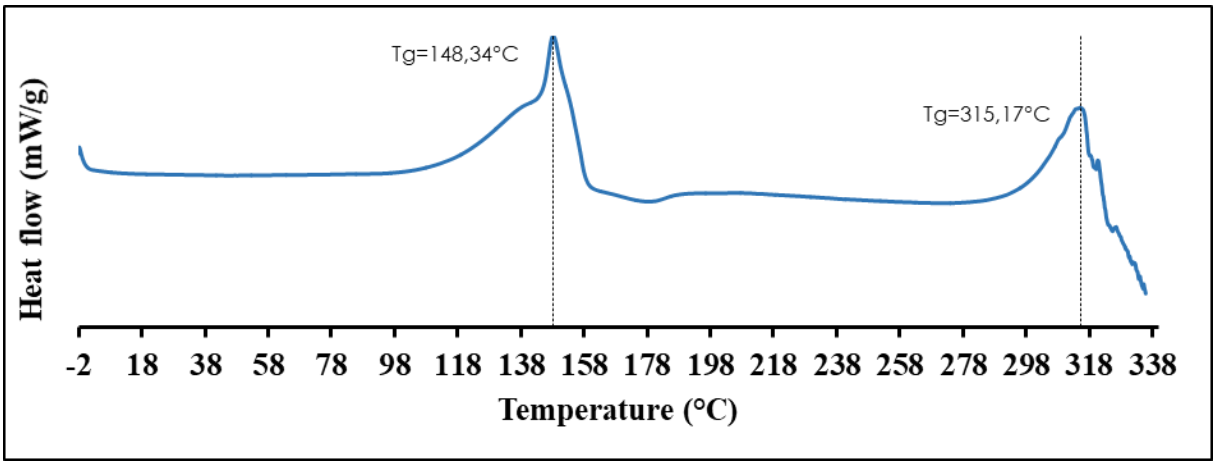

Figure 17: DSC thermogram of ciprofloxacin powder.

4.2.2 X-Ray diffraction of nanofibers

The XRD diffractogram of the pure substances, PCL, MTZ and CPR powders, used for preparation of nanofibers can be seen in Figure 18. The diffractogram of PCL powder indicates semi-crystalline state. The diffractogram is diffused as it is typical for amorphous state, but there are also three wider peaks at 21.5°, 23.9° and 38.2° (Figure 18c). Diffractogram of both drugs revealed their crystallinity with typical sharp and intense peaks: for MTZ at 12.3°, 13.9°, 24.7°, 27.9° and 29.2° (Figure 18a) and for CPR at 8.1°, 8.9°, 19.2° and 26.4° (Figure 18b). Values of diffraction angles are compliant with the literature (70, 75-77).

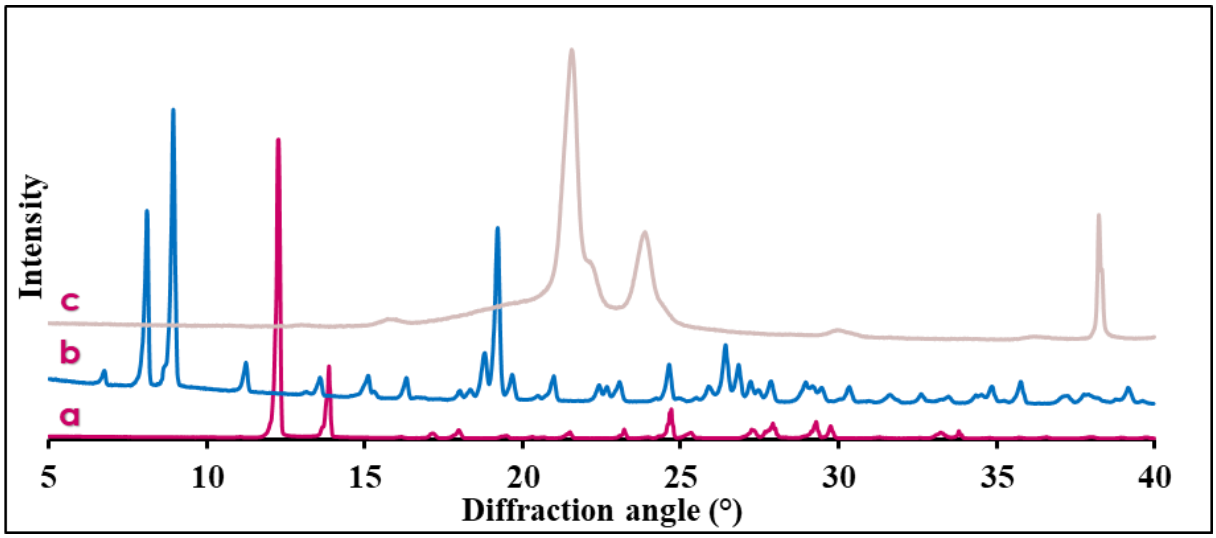

Figure 18: XRD diffractogram of a) metronidazole powder, b) ciprofloxacin powder and c) PCL powder.

To detect the possible change of the physical state of PCL polymer during the electrospinning process, PCL nanofibers without any drugs were compared with PCL powder (Figure 19). The XRD study revealed that diffractograms are very similar with the slightly lower and wider peaks in case of nanofibers compared to a powder. Thus, electrospinning mildly lowered PCL crystallization, which is in line with previous study (78).

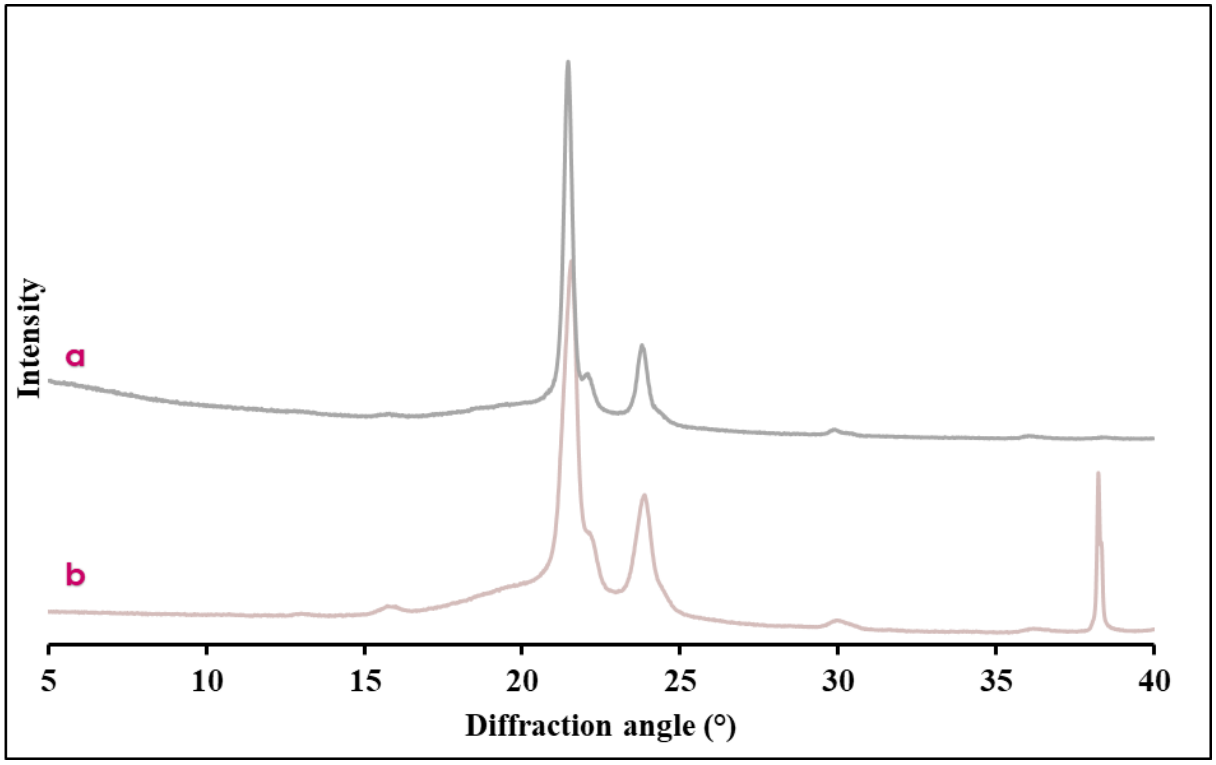

Figure 19: XRD diffractogram of a) PCL nanofibers and b) PCL powder.

Patterns of PCL powder and its physical mixtures with MTZ, CPR or both drugs show typical reflections of components marked with arrows in Figure 20. Intensity of those reflections is smaller according due to the proportion of drugs in the mixture. These powder mixtures were used for comparison understanding the solid state of drugs incorporated in the nanofibers.

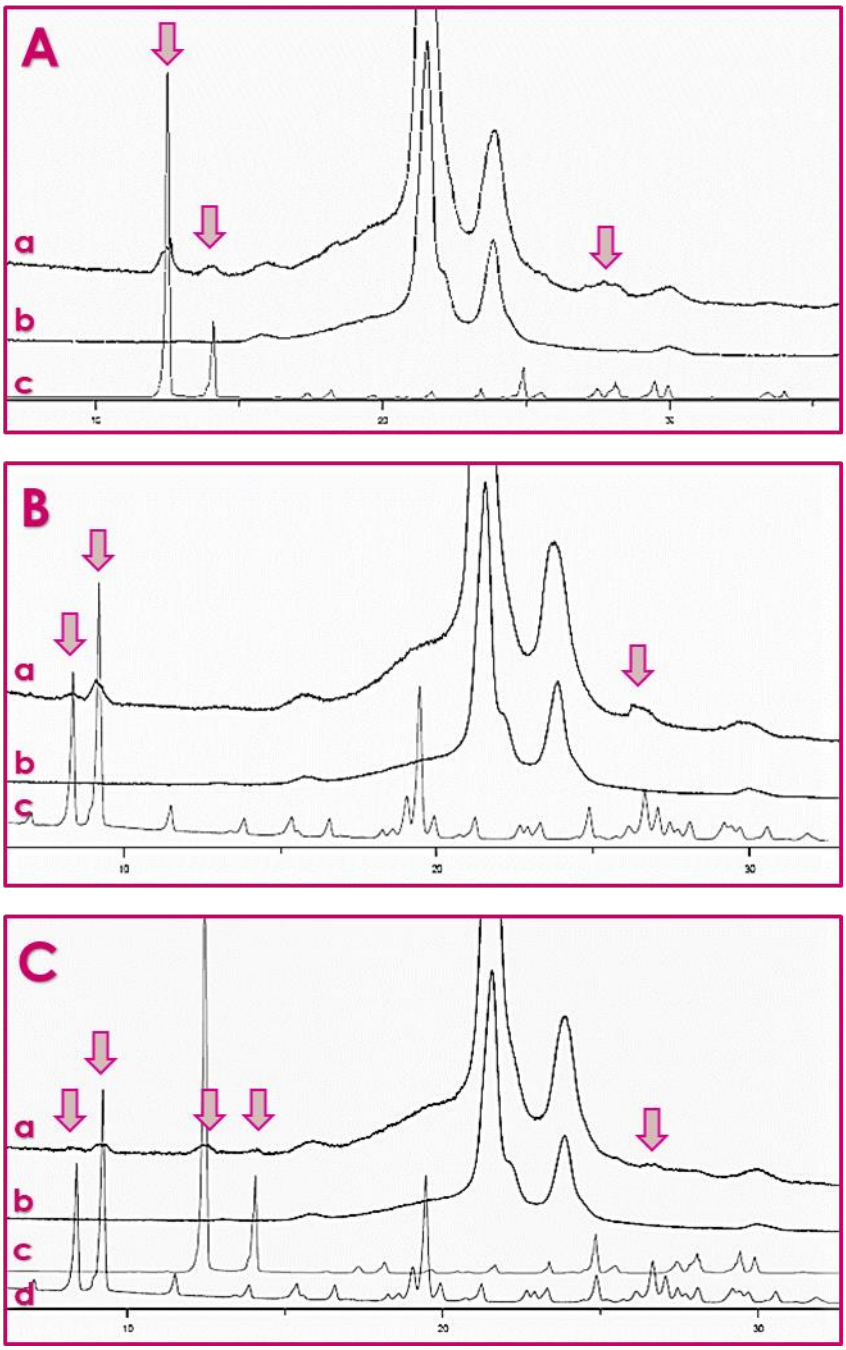

Figure 20: A: Comparison of a) physical mixture of PCL+ metronidazole powder, b) PCL powder, c) metronidazole powder ; B: Comparison of a) physical mixture of PCL+ ciprofloxacin powder, b) PCL powder, c) ciprofloxacin powder, C: Comparison of a) Physical mixture of PCL+ ciprofloxacin + metronidazole powder, b) PCL powder, c) metronidazole powder, d) ciprofloxacin powder.

The characteristic reflections of crystalline MTZ were found in PCL nanofibers with MTZ (Figure 21b), which indicates that drug was in a crystalline state and according to SEM images it was incorporated within the nanofibers (Figure 15B). However, the reflections had lower intensity in case of nanofibers compared to the physical mixture indicating the reduced crystallinity of MTZ. Diffractogram of PCL nanofibers with combination of both drugs (Figure 21c) showed lower MTZ diffraction peaks compared with nanofibers with MTZ (Figure 21b), which correlates with lower quantity of MTZ. Results were comparable in the study of Sahoo et al. (75).

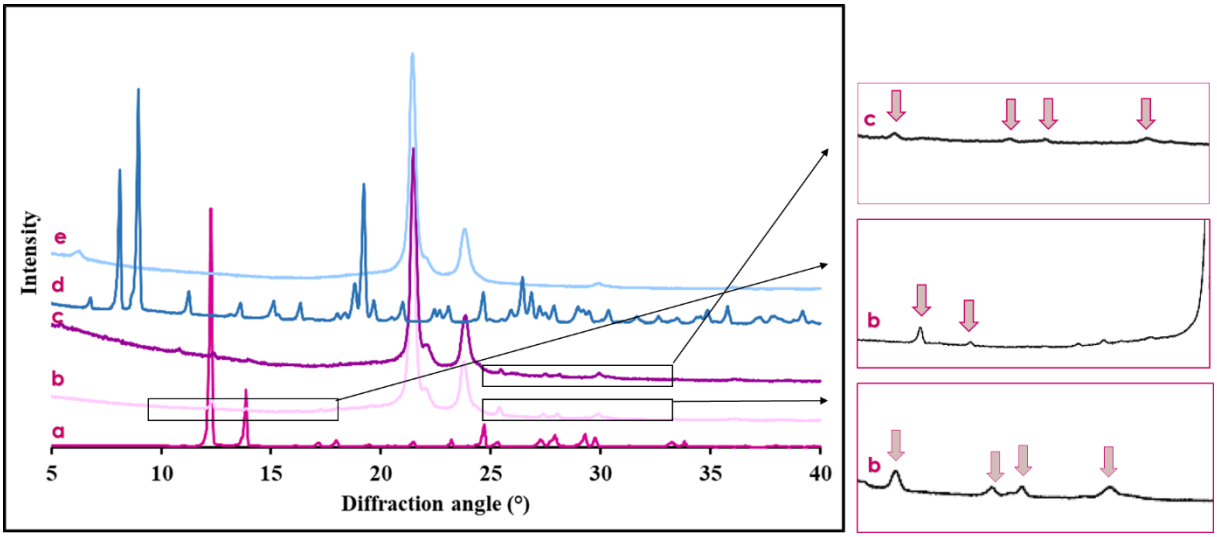

Figure 21: Left: XRD diffractograms of a) metronidazole powder, b) metronidazole nanofibers, c) nanofibers with combination of both drugs, d) ciprofloxacin powder and e) ciprofloxacin nanofibers; Right: marked reflections of crystalline metronidazole in nanofibers.

Characteristic reflections for CPR were not seen in any of nanofibers (Figure 21c, e), therefore CPR may be incorporated in an amorphous form, changed polymorphic structure or as a solvate with organic acids. By contrast, some nanocrystal deposits can be seen in the SEM images in Figure 15C. Because those nanocrystals are in nanoscale, there is a possibility that XRD could not detect them or that the drug is in the amorphous state as stated before. In the study of Demirci et al. they suggested that CPR was incorporated in amorphous state also (79), but in the study of Ignatova et al. they reported crystalline aggregates (80). Both studies have used electrospinning process, but different polymer and solvents for the preparation of polymer solutions were applied.

4.2.3 FTIR spectroscopy of nanofibers

FTIR spectrum of MTZ powder is presented in Figure 22, where we marked the characteristic MTZ peaks, which match with the literature data. Broad peak at 3206 cm^{-1} shows presence of –OH group. 3096 cm^{-1} peak represents alkene monosubstituted CH stretching in the imidazole ring. A signal for C-NO_2 functional group is seen at 1533 cm^{-1}. Two peaks at 1474 and 1425 cm^{-1} exhibit C-C stretching and peak at 1265 cm^{-1} C-N stretching. Absorption peak at 1072 cm^{-1} is present because of the C-O group (72, 81-84).

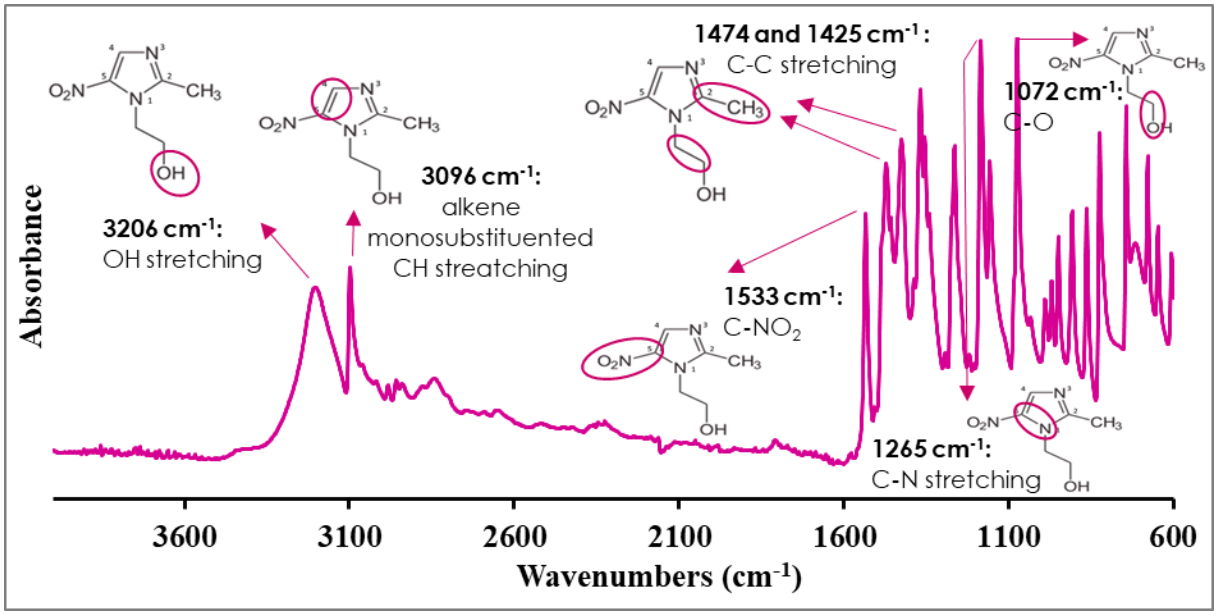

Figure 22: FTIR spectrum of metronidazole with typical peaks.

Figure 23 represents FTIR spectrum of CPR. Typical peaks are marked and when compared to the literature the values of absorbance match. OH-stretching peak occurs at 3526 cm^{-1}. 3372 cm^{-1} peak is typical for tertiary amine and 3090 cm^{-1} for secondary amine. Peak at 1699 cm^{-1} represents carbonyl group and peak at 1616 cm^{-1} is assigned for carboxyl functional group conjugated from phenyl framework. C-F peak appears at 1265 cm^{-1} and C=CH bending peak at 802cm^{-1} (71, 75, 79, 85-88).

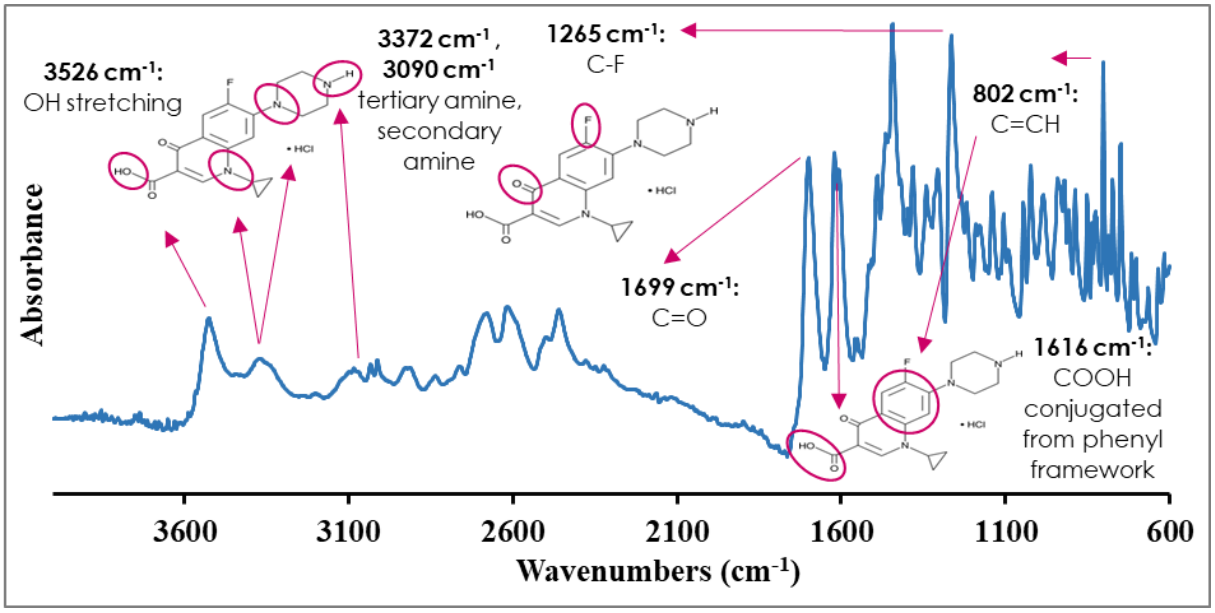

Figure 23: FTIR spectrum of ciprofloxacin with typical peaks.

FTIR spectrum of polymer PCL is shown in Figure 24. Typical peaks were compared with the literature peaks and they match nicely. Two absorption peaks at 2943 and 2866 cm^{-1} represent asymmetrical and symmetrical CH_2 stretching. The sharpest peak at 1728 cm^{-1} is typical for carbonyl group. C-O-C asymmetrical and symmetrical stretching occurs at 1238 and 1163 cm^{-1} (73, 89-93).

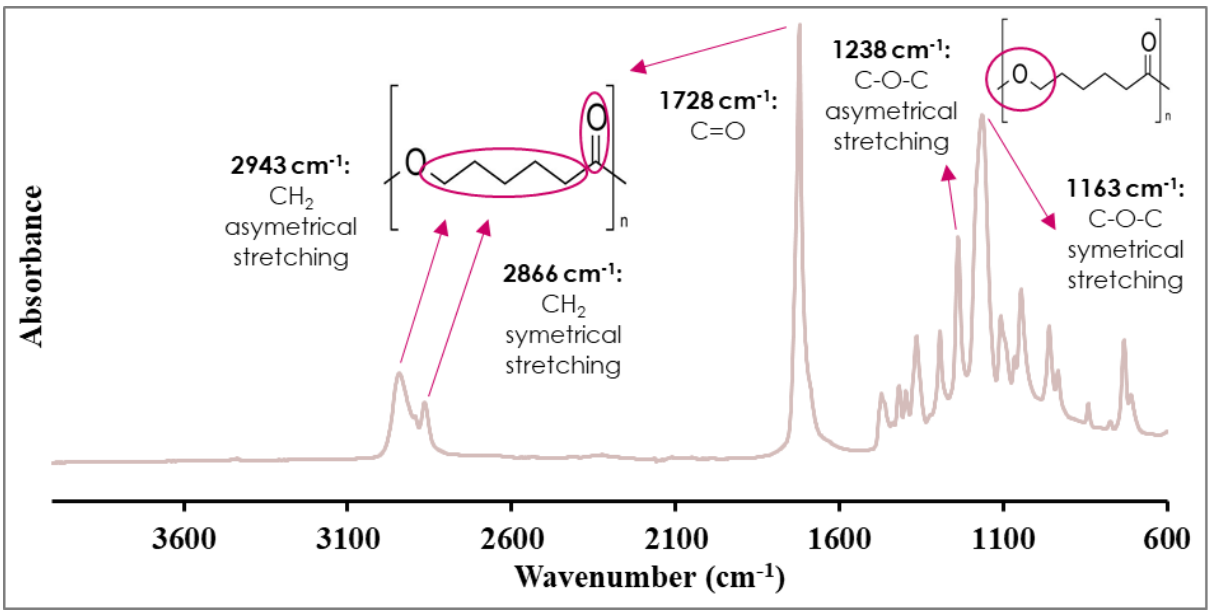

Figure 24: FTIR spectrum of PCL with typical peaks.

Physical mixture of PCL and MTZ (Figure 25d) with the same ratio of the substances as in nanofibers compared to MTZ (Figure 25c) and PCL powder alone (Figure 25a), exhibits typical peaks for MTZ in the mixture. Those peaks that are present in spectrum of physical mixture and are not present in PCL powder spectrum are MTZ peaks. They are less intense due to lower concentration in the mixture and are at the same position as in MTZ powder, so no shift was observed. Most noticeable peaks correspond to alkene monosubtituted CH streatching in the imidazole ring, OH-stretching and presence of NO_2 group (Figure 25; marked with -----). Nanofibers with MTZ (Figure 25e) posess the same peaks as physical mixture of PCL and MTZ, although they are decreased and less intense. That means that MTZ was incorporated in the nanofibers and there was no strong interaction between the polymer and the drug using electorpsinning method. (72, 86).

Comparing CPR powder (Figure 25f), PCL powder (Figure 25a), physical mixture of PCL and CPR (Figure 25g) and CPR nanofibers (Figure 25h) gives us the information about the presence of the drug in the nanofibers and its interaction with the polymer. Ratio of the substances in the physical mixutre is the same as in the nanofibers. The most noticable is the peak that stands for carboxyl group at 1616 cm^{-1} and the peak at 802 cm^{-1} for C=CH bending (Figure 25; marked with - - - -). In spectrum of nanofibers with CPR (Figure 26h) there is a shift of carboxyl peak to higher wavelength (1616 cm^{-1} to 1627 cm^{-1}, marked with arrows in Figure 25). In the study of Demirci et al., they suggested that CPR could interact with the polymer, creating hyrogen bonds. Because this shift happens only at one peak, this sould not affect CPR release (79).

Physical mixture of PCL, MTZ and CPR (Figure 25i) with the same ratio of substances as in nanofibers, exhibits the same spectrum characteristics as physical mixtures with only one drug. Peaks of MTZ and CPR in the mixture are less intense due to the lower amount of the compounds, such as peaks of CH streatching in the imidazole ring and peak for –OH-group of MTZ. Nanofibers with MTZ and CPR (Figure 25j) have also peaks with lower intensity and some of them have disappered. Thus, MTZ and CPR were sucessfuly incorporated in the nanofibers. The only shift observed was carboxyl peak of CPR in case of CPR nanofibers and nanofibers with both drugs due to possible interactions between PCL and CPR.

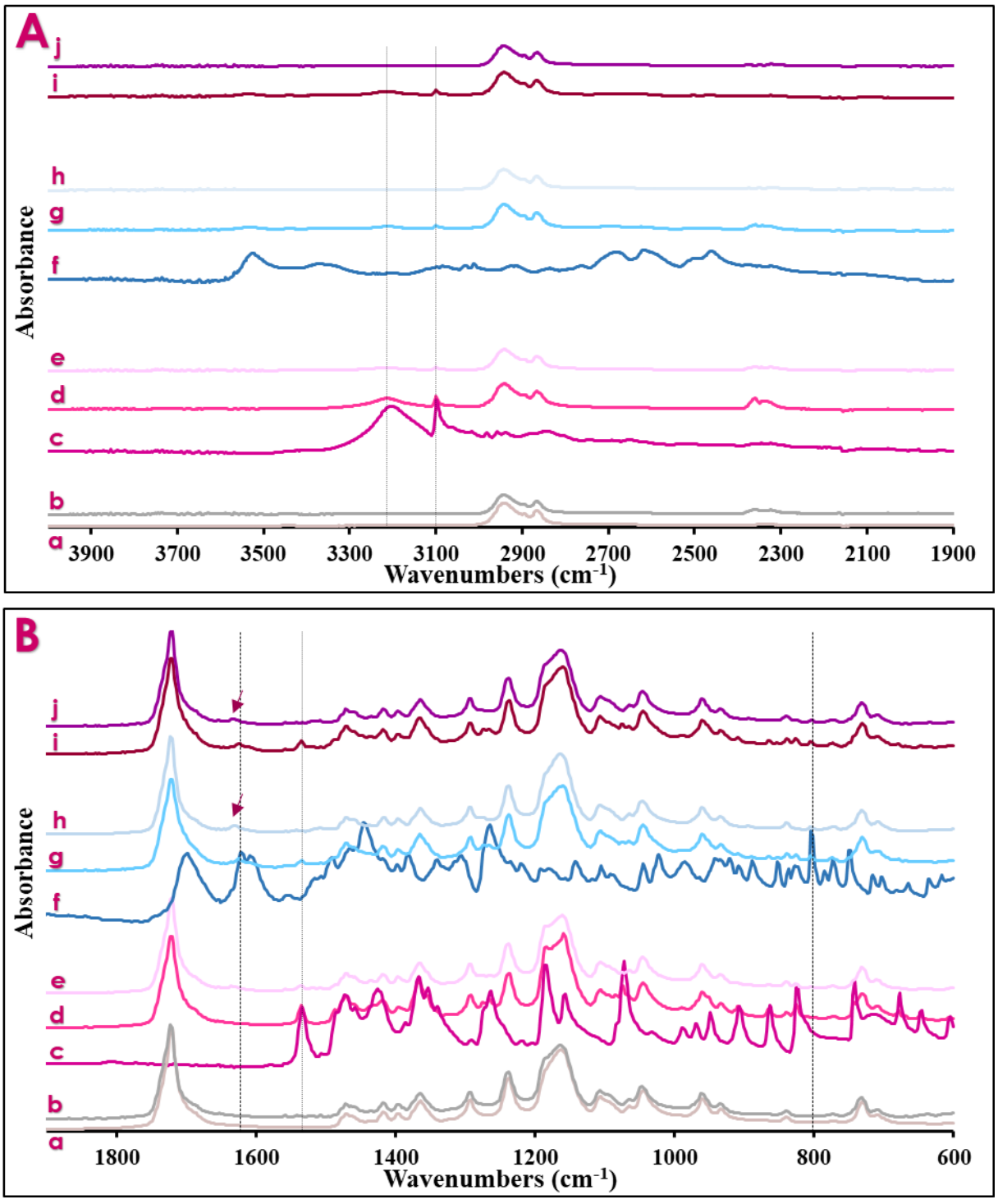

Figure 25: FTIR spectra in range of A) 4000-1900 cm^{-1} and B) 1900-600cm^{-1} of a) PCL powder, b) PCL nanofibers, c) metronidazole powder, d) physical mixture of PCL + metronidazole, e) metronidazole nanofibers, f) ciprofloxacin powder, g) physical mixture of PCL + ciprofloxacin, h) ciprofloxacin nanofibers, i) physical mixture of PCL + ciprofloxacin + metronidazole and j) nanofibers with combination of drugs.

4.3 CIPROFLOXACIN HCl AND METRONIDAZOLE RELEASE FROM NANOFIBERS

Drug release from nanofibers is very important for the development of new delivery systems, which can be modified to achieve the immediate, delayed or prolonged release due to the selection of polymers, drugs and delivery system (94). In the treatment of periodontitis prolonged drug release is desirable together with the drug concentrations above minimal inhibitory concentration (MIC) against targeted periodontal pathogens for a few days to be efficient and reduce the possibility to antibiotic resistance development. Prolonged release is also desirable in the treatment of chronic diseases for better patient compliance to avoid multiple drug administration (59, 95, 96). Consequently, PCL as the representative of hydrophobic polymers was chosen in this study, since it has been often used for prolonged release due to slow drug diffusion from nanofibers (59, 60, 97). Because it is slowly biodegradable, the biodegradability should not play an important role in drug release (98). Release of CPR, MTZ and combination of both from PCL nanofibers was performed in sink conditions with phosphate buffer with pH 7.4, which mimic the pH of the crevice gingival fluid (99), whereas the release volume was significantly bigger compared to *in vivo* conditions (5).

The release profiles of all developed nanofibers here are presented in Figure 26. MTZ released from nanofibers immediately reaching 72% of release in the first half an hour. After that, the amount of drug in the medium remained constant. Compared to the literature 70% of released MTZ from similar mats as PCL fibers was detected after 7 days release study (60, 66, 81). Results did not show prolonged release as expected and reason for burst release can be damaged nanofibers. Hence the medium could diffuse into the nanofibers and MTZ was released into the medium. Other possible explanations are that MTZ was not incorporated into the nanofibers and area in the SEM image was non-representative or MTZ was close to the surface of the nanofibers and therefore easily reachable for media.

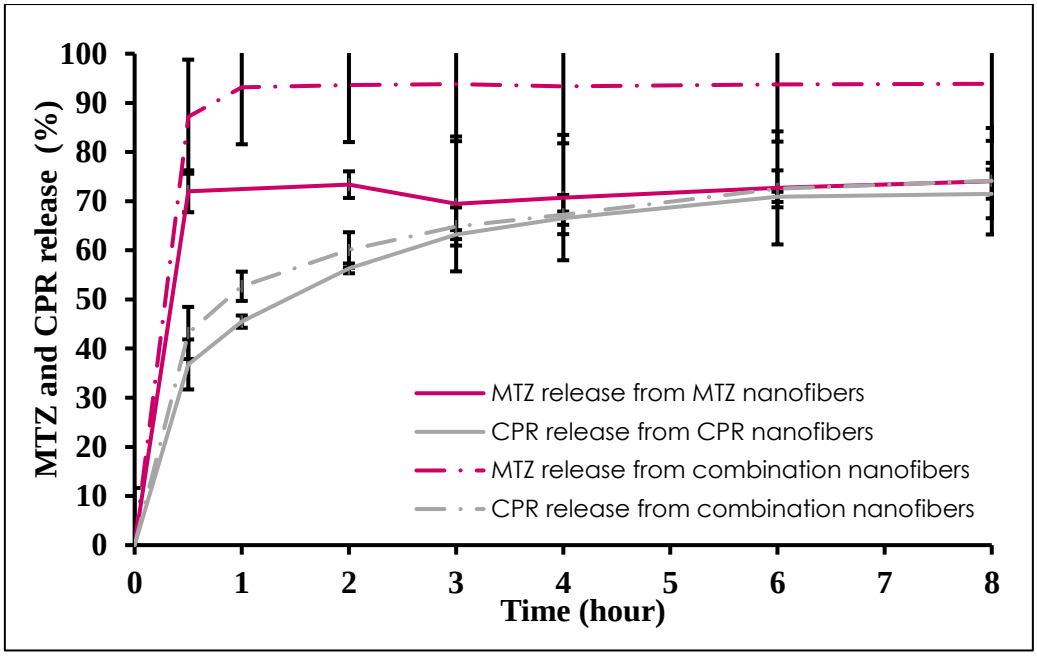

Figure 26: Release profiles of incorporated drugs from metronidazole nanofibers, ciprofloxacin nanofibers and combination nanofibers in eight hours. Data are reported as mean ± SD from three (n=3) parallels.

37% of CPR was immediately released in the first half an hour (Figure 26). After that, prolonged release was obtained up to 6 hours. In the next hours concentration of CPR was constant approximately 60%. In this case burst release profile nicely correlates with SEM images, where crystals of the CPR can be seen on the nanofibers. The drug was not incorporated into the nanofibers and consequently, it was easily accessible to the medium. Comparing CPR profile with MTZ profile, release in the first half an hour is slower with CPR which is the case in line with literature. However, the total concentration percentage of both released drugs is lower. For example, amount of MTZ and CPR alone released in the first 8 hours were approximately 30% and 10% in study of Bottino et al. (65, 66). Dang et al. studies even showed such prolonged release that 40% of MTZ and 10% of CPR was released after 24 hours and in Puga et al. study less than 50% of CPR in 3 months. The reason for such subsequent slowdown in release rate in Puga's study could be attributed to drug entrapped in the PCL matrix, which had to dissolved and diffused through the pores (100, 101).

Release of CPR from nanofibers with the combination of both drugs (Figure 26) is comparable to the release profiles obtained from CPR nanofibers, whereas MTZ release from

nanofibers with combination of both drugs was faster than from MTZ nanofibers. SEM image shows (Figure 15D) nanocrystals on nanofiber surface which explains and correlates with the obtained burst release of both drugs. Figure 27 represents the same release profiles as in Figure 26 but in different time range of 5 days. Concentrations of both released drugs in the medium remained constant for all nanofibers, although concentration of MTZ from nanofibers with only MTZ slightly increased after 4 days.

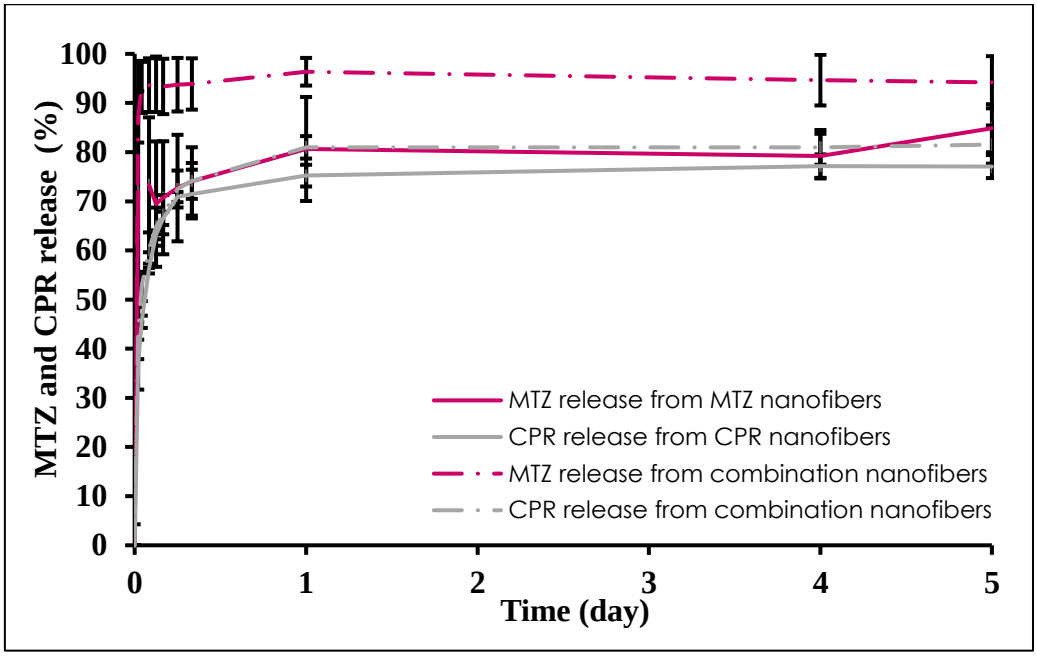

Figure 27: Release profiles of incorporated drugs from metronidazole nanofibers, ciprofloxacin nanofibers and combination nanofibers in five days. Data are reported as mean ± SD from three (n=3) parallels.

The electrospinning process enabled the incorporation of the drugs in the nanofibers or onto their surface, nanofibers released drug immediately and thus, they could be used for short but not for prolonged treatment of periodontitis.

4.4 CYTOTOXICITY OF NANOFIBERS ON FIBROBLASTS

Since nanofibers could be used as a new drug delivery system for the treatment of periodontal disease, they should be made from safe, nontoxic and biocompatible material. PCL is US Food and Drug Administration (FDA) and European medicines agency (EMA) approved polymer (101-104). In this study nanofibers cytotoxicity was tested according to standard cytotoxicity tests since nanotoxicity standards have not been yet recognized by ISO (105). The

main difference between cytotoxicity and nanotoxicity is the size of tested material. The way organism respond to the exposure of the material is largely effected by particle size (106).

In Figure 28, the results of BHK fibroblasts viability from direct and indirect method is shown. Direct method gave us results of the viability of fibroblasts, which grew in the media together with nanofibers. Indirect method is different in that way, that nanofibers were soaked in the media first, removed and then the fibroblasts were transferred into the media. Comparing direct and indirect method the average viability of tested fibroblasts is almost the same: 75.8% in direct method and 75.6% in indirect method (Table I in Supplement). However, the standard deviation is higher in indirect method. The analysis with T-test showed no statistically significant differences between the methods. The highest viability with both methods was achieved with PCL nanofibers with combination of both drugs. Average viability of fibroblasts in negative control from both methods was 75%. In case of positive control, the number of live and dead cells was below detection limit which means, that almost every cell was dead and viability was 0%.

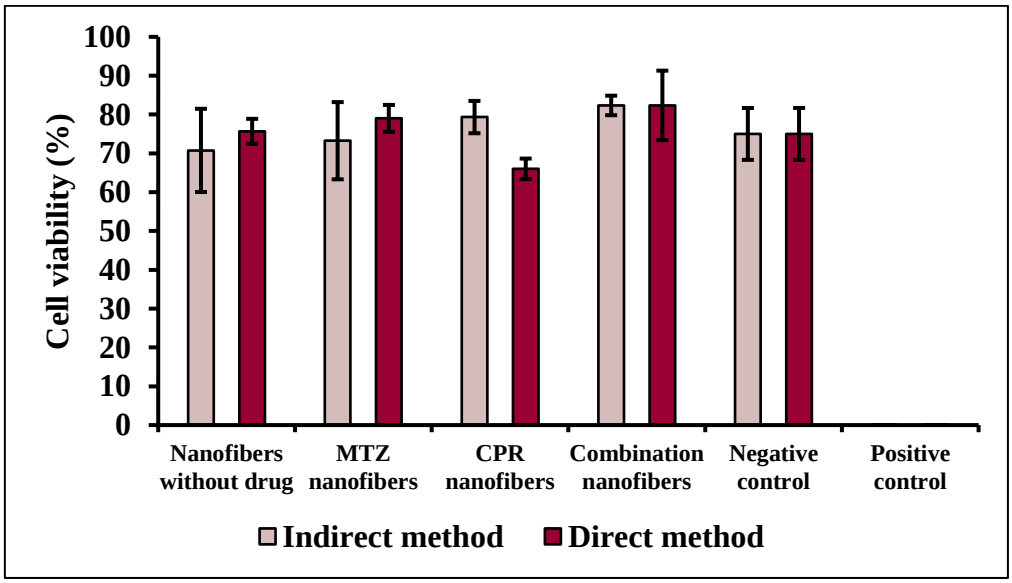

Figure 28: Cell viability of BHK fibroblast with nanofibers without drug, metronidazole, ciprofloxacin and combination nanofibers, positive and negative control.

In Figure 29, there is a comparison of morphology between live and dead fibroblast. Density of live cells is really high and consequently, the typical dendritic shape of fibroblasts cannot be clearly seen. Round shapes in the images represent dead cells which detached from

the well and are free floating in the medium. Live fibroblasts are in elongated shape attached to the bottom of the well (106, 107). There is no difference between different samples of nanofibers and a negative control.

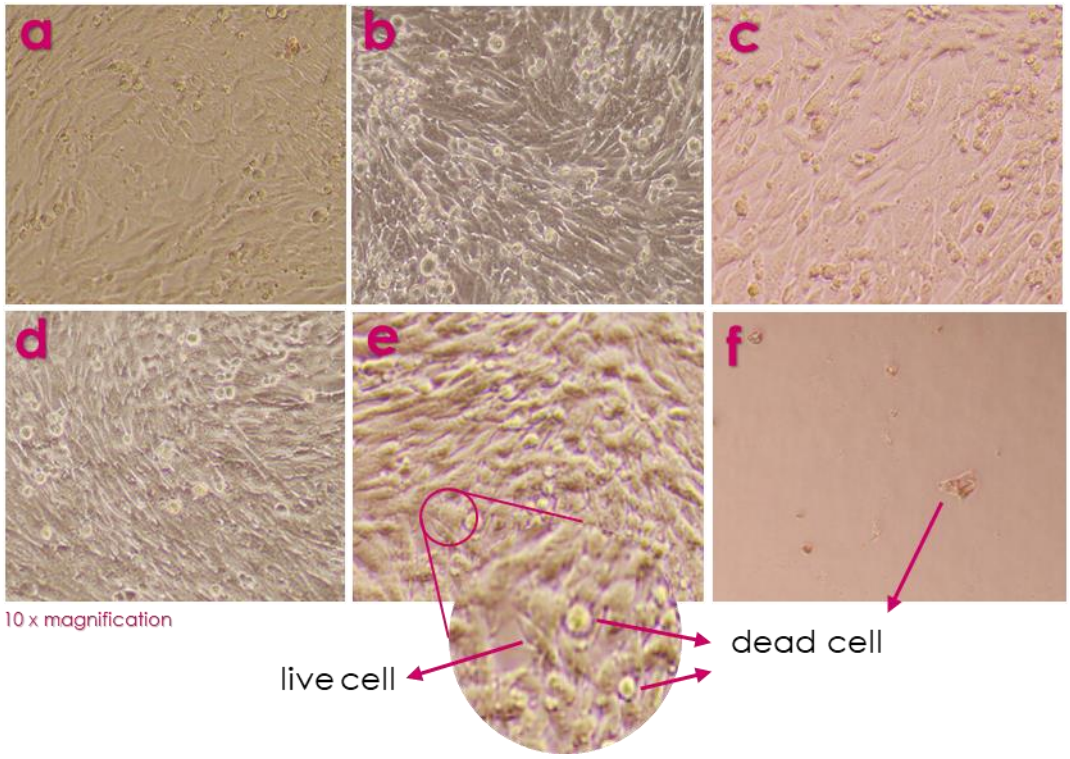

Figure 29: Morphology of live and dead BHK fibroblasts treated with a) nanofibers without drug b) metronidazole nanofibers, c) ciprofloxacin nanofibers, d) combination nanofibers, e) negative control and f) positive control.

According to ISO standard 10993-5 the cytotoxicity of the material can be evaluated qualitative and quantitative. Qualitative observation covers cell's morphology changes. If there is not more than 20% of the cells detached or slightly attached, with changed morphology and only a few lysed, the test material is slightly cytotoxic. Higher number of dead cells means that material could be slightly, mildly or moderately cytotoxic. It must be notated that non-toxic materials also exist and in that case there is no cell lysis or reduction of growth present (63). Fibroblasts in case of all our nanofibers showed small changes in morphology such as detachment and lysis which could indicate slight cytotoxicity, but same changes were also seen in the negative control, because cells start to detach if they have no more space to grow. Percentage of the dead cells was not significantly different from negative control and there is a possibility that low viability is the consequence of technical handling of samples and not the

cytotoxicity of the nanofibers itself. Quantitative analysis was performed with coloring the dead cells with trypan blue so machine can count them. Some of them could also die because of the coloring. Relevant studies, where PCL nanofibers of other form of PCL polymer were observed for cytotoxicity, claim that material is safe if cell viability is above 80% and some even 60%. All the given studies with ISO guided tests concluded that PCL is not cytotoxic and it is safe to use (104, 108-110). In the study of Murguia et al. the viability of the human dental pulp stem cells treated with PCL scaffolds even after 14 days was still around 60% (103). Although our test was not run for more than two days, the conclusion is that viability was the same in all tested material as in negative control which indicates that PCL nanofibers are safe. However, further nanotoxicity studies should be considered, especially long-term studies where contact of gums with nanofibers is imitated.

4.5 ANTIBACTERIAL ACIVITY OF NANOFIBERS

Disk diffusion assay was used to determine qualitative efficacy of drugs incorporated into the nanofibers against periodontal pathogens *P. gingivalis, F. nucleatum, S. mutans, A. Actinomycetemcomitans* and *E.coli.* If the drugs were stable during storage and then released from nanofibers in sufficient amount to kill bacteria, the inhibition zones were observed (42).

4.5.1 Porphyromonas gingivalis

The results of disk diffusion assay on *P. gingivalis* is presented in Figure 30. Inhibition zone can be seen in Figure 30a and b where efficacy of the nanofibers with MTZ and MTZ positive control can be seen (- - - -). In Figure 30c and d are presented inhibition zones for nanofibers with CPR and CPR positive control (- - - -). Bottino's study of CPR and MTZ efficacy against *P. gingivalis* reported similar results. Drugs were incorporated in the same concentrations in polydioxanone monofilaments as in our nanofibers and used in disk diffusion assay. Inhibition zones were comparable. MTZ mats presented bigger inhibition zones than CPR mats which was also the case in our study (66). Very dark bacteria in Figure 31e are indicated as *P. gingivalis*, whereas gray circle around disk is suggested as fungal infection (Figure 30c, d - - - -) (111). Figure 30e represents plate with negative controls.

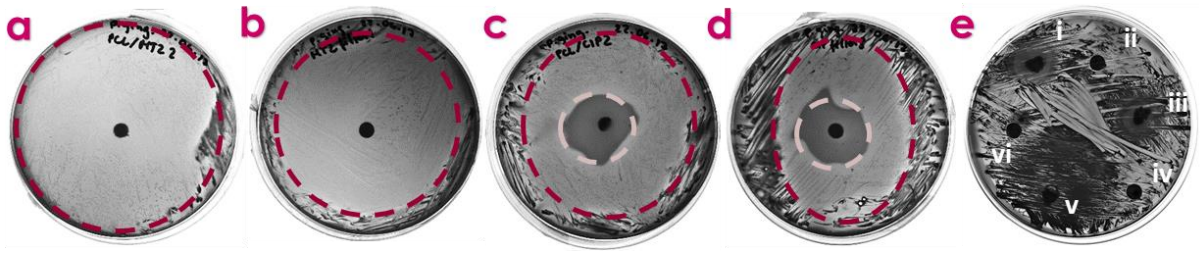

Figure 30: Inhibition zones of a) metronidazole nanofibers b) metronidazole positive control, ciprofloxacin nanofibers, d) ciprofloxacin control and e) i, iii, v: nanofibers without drug and ii, iv, vi: filter paper on *P. gingivalis.*

4.5.2 Fusobacterium nucleatum

Figure 31a and b represent efficacy of MTZ nanofibers and MTZ positive control and it can be concluded that nanofibers with MTZ are more effective against *F. nucleatum* than nanofibers with CPR (Figure 31c i). Figure 31c ii shows negative control and 31c iii CPR positive control. In Figure 31d inhibition zone around disk appeared due to the released MTZ and CPR from nanofibers with combination of drugs. Therefore, these work more or less the same as nanofibers with MTZ. Positive control of combination of both drugs is presented in Figure 31e. Bottino and his coworkers performed a study where diameter against *F. nucleatum* was assessed using different polymer nanofibers with the same amount of MTZ and CPR incorporated. Inhibition zone appeared with nanofibers with CPR, but did not appear with nanofibers with MTZ (66). In Reise et al. study, MTZ nanofibers were efficient against *F. nucleatum* as well (112).

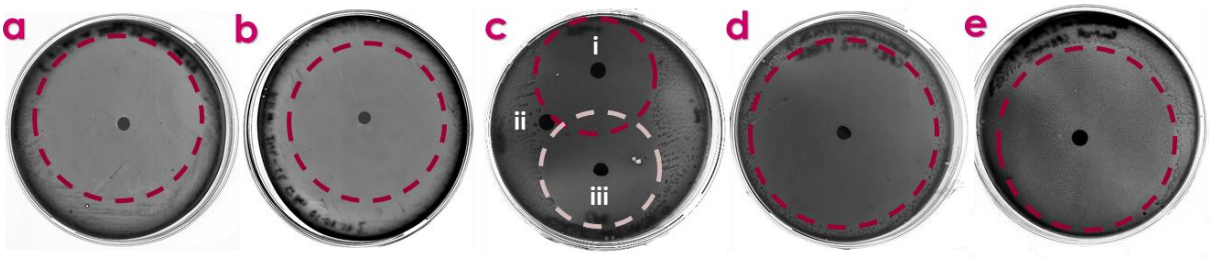

Figure 31: Inhibition zones of a) metronidazole nanofibers, b) metronidazole positive control, c) i: ciprofloxacin nanofibers, ii: filter paper, iii: ciprofloxacin positive control, d) nanofibers with combination of drugs and e) metronidazole + ciprofloxacin positive control on *F. nucleatum.*

4.5.3 Streptococcus mutans

Figure 32 represents disk diffusion assay on *S. mutans*. MTZ nanofibers (Figure 32a i) as well as its positive control (Figure 32c i) are not efficient against *S. mutans* and it can be concluded that this bacterial strain is resistant against MTZ in its used concentrations (39). There is one inhibition zone around the nanofibers with CPR (Figure 32a ii) and one around positive control of CPR (Figure 32 c ii). In Figure 32b are visible inhibition zones around nanofibers with combination of drugs (i) and positive control of drug combination (ii), whereas there are no inhibition zones around PCL nanofibers without any drug (iii) and negative control (iv). Inhibition zones around nanofibers with combination of both drugs are smaller due to lower concentration of CPR incorporated. Comparable results of CPR efficacy appeared in Chowdaiah and Dhamodhar's study (40). In the study of Johnston et al., nanofibers made from different polymers with CPR in combination with diclofenac but in the same concentration showed inhibition zones as well (42).

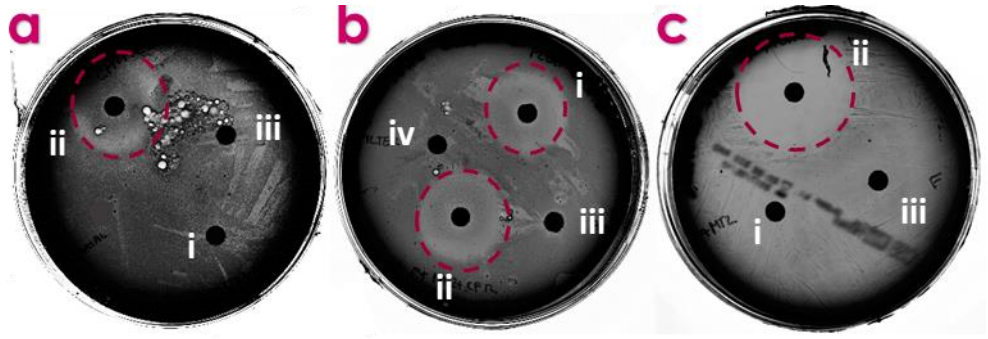

Figure 32: Inhibition zones of a) i: metronidazole nanofibers, ii: ciprofloxacin nanofibers, iii: filter paper, b) i: nanofibers with combination of drugs, ii: metronidazole + ciprofloxacin positive control, iii: nanofibers without drug, iv: filter paper and c) i: metronidazole positive control, ii: ciprofloxacin positive control, iii: filter paper on *S. mutans*.

4.5.4 Aggregatibacter actinomycetemcomitans

Disk diffusion assay with *A. actinomycetemcomitans* is presented in Figure 33. MTZ nanofibers (Figure 33a i) are effective against bacteria but comparing with CPR nanofibers (Figure 33a ii) way less. Difference in diameters of the inhibition zone is smaller in positive controls of MTZ (Figure 33c i) and CPR (Figure 33c ii). Figure 33b presents results from nanofibers with combination of drugs (i) and positive control of combined drugs (ii) Diameter

is the same as in nanofibers with CPR and positive control of CPR and it can be concluded that effect of the CPR is dominant and combination with MTZ in nanofibers does not improve efficacy against *A. actinomycetemcomitans*. The third inhibition zone in Figure 33b iv is around PCL nanofibers without any drug. Comparing these nanofibers with negative control, where there was no inhibition zone in any plate and in any bacteria, there is a possibility that *A. actinomycetemcomitans* is sensitive even to the PCL material. Since inhibition zone was twice as big as in nanofibers with MTZ which are also from PCL material that could not be the case. Another possible explanation could be that CPR diffused from nanofibers with combination of drugs and PCL nanofibers without any drug, pulled the drug towards itself, soaked CPR and consequently acted as nanofibers with CPR. There is also possibility that some of the solvents for solution of PCL and the drugs remained in nanofibers and killed the bacteria. Bottino et al. suggested comparable results with different polymer for nanofibers but with the same concentration of MTZ and CPR (66).

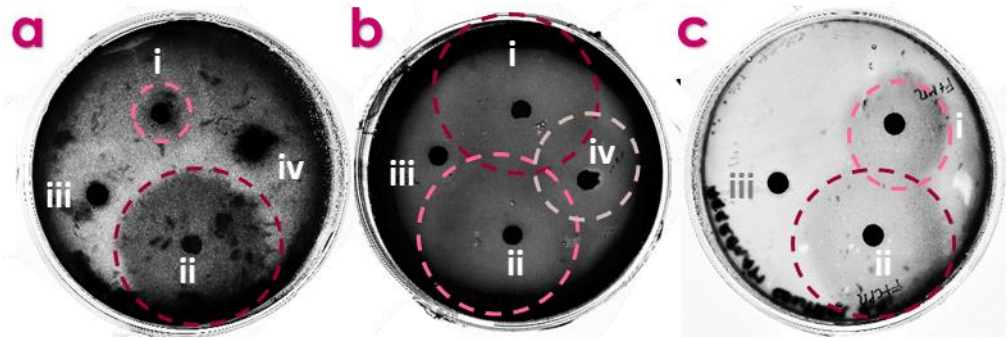

Figure 33: Inhibition zones of a) i: metronidazole nanofibers, ii: ciprofloxacin nanofibers, iii: filter paper, iv: nanofibers without drug, b) i: nanofibers with combination drugs, ii: metronidazole + ciprofloxacin positive control, iii: filter paper, iv: nanofibers without drug and c) i: metronidazole positive control, ii: ciprofloxacin positive control, iii: filter paper on *A. actinomycetemcomitans*.

4.5.5 Escherichia coli

In Figure 34 are images of anaerobic disk diffusion assay performed on *E.coli*. This disk diffusion assay was the only one performed in aerobic and anaerobic conditions, since *E. coli* is facultative anaerobe. Figure 34a shows MTZ nanofibers (i), CPR nanofibers (ii), nanofibers without any drug (iv) and negative control (iii). Nanofibers with combination of drugs are presented in Figure 34b i where are also positive control of combination of the drugs (ii),

negative control (iii) and nanofibers without any drug (iv). In the last plate (Figure 34c) are both positive controls of the drugs (i, ii) and negative control (iii). Inhibition zones appeared only there, where CPR was present. Results were confirmed with Johnston et al. study (42). Comparing anaerobic and aerobic results, there was no difference observed.

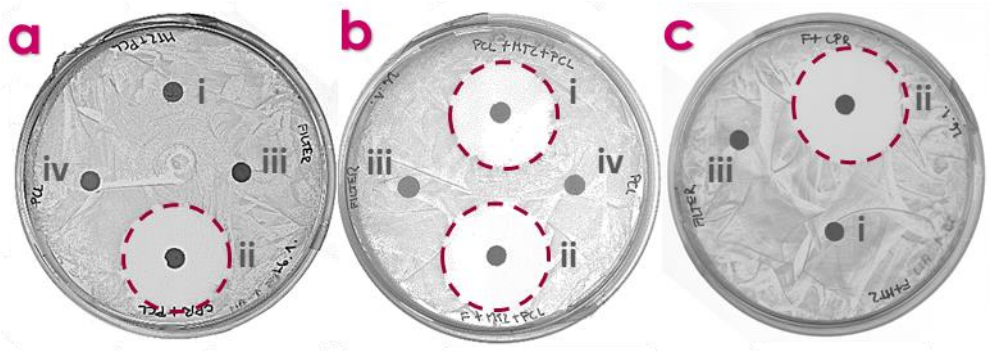

Figure 34: Inhibition zones of a) i: metronidazole nanofibers, ii: ciprofloxacin nanofibers, iii: filter paper, iv: nanofibers without drug, b) i: nanofibers with combination of drugs, ii: metronidazole + ciprofloxacin positive control, iii: filter paper, iv: nanofibers without drug and c) i: metronidazole positive control, ii: ciprofloxacin positive control, iii: filter paper on *Escherichia coli*.

4.5.6 Comparison of antibacterial activity of all nanofibers on all tested periodontal pathogens

PCL nanofibers containing MTZ worked against *P. gingivalis*, *F. nucelatum*, and *A. actinomycetemcomitans* with the highest diameter values of inhibition zones in that order. PCL nanofibers containing CPR showed antibacterial activity against all tested bacteria. The biggest inhibition zone was observed against *P. gingivalis*, followed by *F. nucleatum*, *A. actinomycetemcomitans* and *S. mutans*. PCL fibers with combination of both drugs showed biggest inhibition zone against *P. gingivalis* (Figure 35). Considering that both MTZ and CPR alone worked most effective against *P. gingivalis*, such result was expected. Although concentrations of both drugs were lower in nanofibers with combination of drugs, that could be indication of additive activity of both drugs. Combination of MTZ, CPR and minocycline was proved to be clinically effective with endodontic treatment in the study of Takushige et al. Results from Sato et al. also showed better function against periodontal pathogens with the same drug combination. Both studies used ointment as a drug delivery system (113, 114). Windley and his coworkers used paste with those antibiotics and they suggested that mixture of

antibiotics is also beneficial because of the diversity of periodontal bacteria and its different drug resistance (115). Values of diameter zones of PCL nanofibers with combination of drugs coincide with values of nanofibers with one drug. Positive controls showed the same result as nanofibers and there was no statistically significant difference between the control and tested material. Negative controls gave expected results and no inhibition zone was observed.

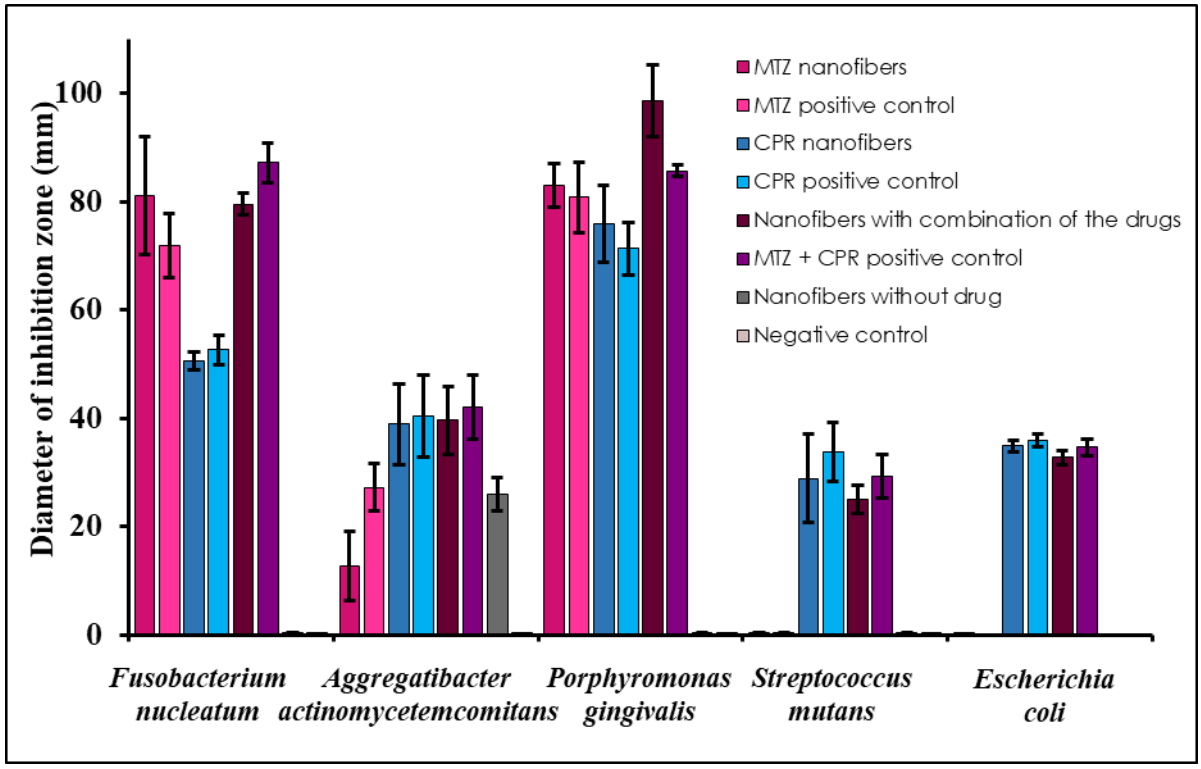

Figure 35: Measured inhibition zones of nanofibers, positive and negative control in *F. nucleatum, A. actinomycetemcomitans, P. gingivalis, S. mutans and E. coli* presenting the antibacterial efficacy of the prepared drug-loaded nanofiber mats.

5 CONCLUSIONS

Four types of nanofibers were prepared with electrospinning method from PCL polymer: PCL nanofibers without drugs and with 5% (w/w) of MTZ, 5% (w/w) of CPR and combination of both with 2.5% (w/w) of drug loading of each. Average diameter of PCL nanofibers without any drug was 502 ± 302 nm. Average diameter of the nanofibers with MTZ, CPR and combination of both was 412 ± 337 nm, 650 ± 356 nm and 1274 ± 481 nm, respectively. SEM images revealed uniform, continuous and beadless nanofibers with MTZ and PCL nanofibers without any drug, while nanofibers with CPR and combination of the drug contained some nanocrystals deposed. Diameter and homogeneity should be further optimized with solution, process and ambient conditions of electrospinning.

DSC thermal analysis showed no drug and polymer interactions and no electrospinning effect on chemical or physical changes. XRD diffractograms revealed that PCL powder was in semi-crystalline state and electrospinning lowered level of crystallinity of PCL. MTZ was incorporated in crystalline state in nanofibers and electrospinning also decreased drug crystallinity. CPR was probably incorporated in an amorphous state or XRD method could not detect nanocrystals due to their nanoscale size. FTIR studies showed no interaction between MTZ and PCL polymer in nanofibers, while CPR and PCL slightly interact with each other creating hydrogen bonds. This did not affect CPR release.

Burst release of MTZ from nanofibers up to 72% in first half an hour was observed. Burst release was also present in case of nanofibers with CPR although it was slower compared to nanofibers with MTZ. Release of CPR from nanofibers with combination of both drugs is comparable with the release profiles from nanofibers with CPR, whereas MTZ release is faster. Reasons for fast release may be damaged nanofibers or too low amount of PCL, which could not sustain the MTZ release.

Viability of BHK fibroblasts tested with direct and indirect methods in case of nanofibers with MTZ, CPR and combination of both as well as blank nanofibers was not statistically different compared to a negative control. Therefore, the nanofibers were not cytotoxic on BHK fibroblasts. Since method was performed according to the standard ISO cytotoxicity tests, nanotoxicity should be examined more carefully with different methods.

Nanofibers with CPR were effective against all tested bacteria strains with the widest inhibition zone against *P. gingivalis*, followed by *F. nucleatum, A. actinomycetemcomitans* and *S. mutans.* Nanofibers with MTZ were not efficient against *S. mutans*. The widest inhibition zone occurred against *P. gingivalis* and *F. nucleatum*. Diameters of inhibitions zones against *P. gingivalis* and *A. actinomycetemcomitans* were wider with nanofibers with MTZ compared to nanofibers with CPR. Nanofibers with the combination of both drugs showed efficacy against bacteria comparable to nanofibers with only one drug incorporated and inhibition zone was as wide as in the case of nanofibers with more effective drug on the specific strain. To sum up, the disk diffusion assay performed on different periodontal pathogenic bacteria showed that nanofibers with combination of both antibacterial drugs are the optimal choice for an antibacterial effect.

After optimizing nanofibers with antimicrobial drugs as a new drug delivery system for the treatment of periodontal disease on desirable level, the next step in testing are *in vivo* studies on animal models. After that, clinical trials should be considered.

6 REFERENCES

1. Linde J, Lang NP, Karring T: Clinical Periodontology and Implant Dentistry (5th edition), Blackwell Publishing company, Oxford, 2008: 185-187, 414, 420-422, 426
2. http://meadfamilydental.com/wp-content/uploads/2015/02/Mandible-labelled.jpg, https://www.infodentis.com/tooth-anatomy/supporting-structure.php, last seen: 2.1.2018
3. Hojo K, Nagaoka S, Ohshima T, Maeda N: Bacterial Interactions in Dental Biofilm Development, Journal of Dental Research. 2009; 88(11): 982-990.
4. Summit JB, Robbins JW, Hilton TJ, Scwartz RS: Fundamentals of operative dentistry, a contemporary approach (3rd edition), Quintessence Publishing Co, Inc, USA, 2006; 25-28
5. Goodson, J M: Gingival crevice fluid flow. Periodontology 2000. 2003; 31: 43-54.
6. http://burton.pro/dentistry/advice/gum-disease-gingivitis-periodontitis/, last seen: 2.1.2018
7. Slovenski medicinski slovar Medicinske fakultete, Univerze v Ljubljani (2012-2018): http://www.termania.net/slovarji/slovenski-medicinski-slovar/5529710/obloga?query=dentalni+plak&SearchIn=All, last seen: 4.1.2018 http://www.termania.net/slovarji/slovenski-medicinski-slovar/5541878/dna-topoizomeraza?query=DNA-giraza&SearchIn=All, last seen: 7.1.2018
8. Zupančič Š, Kocbek P, Petelin M, Kristl J.: Nanozdravila za lokalno zdravljenje parodontalne bolezni. Farmacevtski vestnik 2016; 67: 303–309.
9. Brooks GF, Carroll KR, Butel JS, Morse SA, Mietzner TA: Jawtz, Melnick & Adelberg's Medical Microbiology (26th), The McGraw-Hill Companies, Inc., USA; 2010(10): 169-171
10. http://cariology.wikifoundry.com/photo/7832466/Dental+pellicle+and+formation+of+mature+plaque, last seen: 2.1.2018
11. Bidault P, Chandad, Grenier, D.: Systemic Antibiotic Therapy in the Treatment of Periodontitis, Journal of the Canadian Dental Association, 2007; 73(6): 515–520.
12. Preem L, Mahmoudzadeh M, Putrins M, Meos A, Laidmäe I, Romann T, Aruvali J, Harmas R, Koivuniemi A, Bunker A, Tenson T, Kogermann, K: Interactions between chloramphenicol, carrier polymers and bacteria – implications for designing electrospun

drug delivery systems countering wound infection, Molecular Pharmaceutics, 2017; 14(12): 4417–4430

13. Centralna baza zdravil: http://www.cbz.si, JAZMP-IB/001-13.11.2015, JAZMP-IB/019G-19.4.2018; last seen: 9.6.2018
14. Salahuddin A, Agarwal SM, Avecilla F, Azam A: Metronidazole thiosalicylate conjugates: Synthesis, crystal structure, docking studies and antiamoebic activity, Bioorganic & Medicinal Chemistry Letters, 2012; 22: 5694–5699
15. O'Neil, MJ: The Merck Index - An Encyclopedia of Chemicals, Drugs, and Biologicals. 13th Edition, Merck and Co., Inc., USA; 2001: 1095-96
16. Erah PO, Goddard AF, Barrett DA, Shaw PN, Spiller RC: The stability of amoxycillin, clarithromycin and metronidazole in gastric juice: relevance to the treatment of *Helicobacter pylori* infection, Journal of Antimicrobial Chemotherapy 1997; 39: 5–12
17. Osol A, Hoover JE: Remington's Pharmaceutical Sciences (15^{th}), Mack Publishing Co., USA; 1975: 1161
18. Wu Y, Fassihi R: Stability of metronidazole , tetracycline HCl and famotidine alone and in combination. International Journal of Pharmaceutics 290; 2005: 1–13.
19. Tolls J: Sorption of Veterinary Pharmaceuticals in Soils: A Review, Environmental Science & Technology 2001; 35(17): 3397-406
20. Tally FP, Sutter VL, Finegold, SM: Metronidazole Versus Anaerobes In Vitro Data and Initial Clinical Observations, California Medicine 1972; 17:22-26
21. Niokhor D, Khelaifia S, Lagier JC, Raoult D: The aerobic activity of metronidazole against anaerobic bacteria, International Journal of Antimicrobial Agents 2015; 45(5): 537 – 540
22. Prakasam A, Elavarasu SS, Natarajan RK: Antibiotics in the management of aggressive periodontitis. Journal of Pharmacy & Bioallied Sciences 2012; 4(2): 252–255
23. Gamboa F, Acosta A, García D, Velosa J, Araya N, Ledergerber R: Occurrence of *Porphyromonas gingivalis* and its antibacterial susceptibility to metronidazole and tetracycline in patients with chronic periodontitis, Acta Odontologica Latinoamericana 2014; 27(3):137-44

24. Pankuch GA, Appelbaum PC: Activities of Tizoxanide and Nitazoxanide Compared to Those of Five Other Thiazolides and Three Other Agents against Anaerobic Species, Antimicrobial Agents and Chemotherapy 2006; 50(3):1112-1117
25. Aldridge KE, Ashcraft D, Cambre K, Pierson CL, Jenkins SG, Rosenblatt JE: Multicenter Survey of the Changing In Vitro Antimicrobial Susceptibilities of Clinical Isolates of *Bacteroides fragilis* and *Peptostreptococcus Species*, Antimicrobial Agents and Chemotherapy 2001 45(4):1238-1243
26. Van Winkelhoff AJ, Rurenga P, Singadji Z: Metronidazole and amoxicillin susceptibility of *Aggregatibacter actinomycetemcomitans*, International Journal of Antimicrobial Agents 2014; 43(5): 475–476
27. USP monograph of Ciprofloxacin HCl: http://www.pharmacopeia.cn/v29240/usp29nf24s0_m17870.html, last seen: 9.6.2018
28. Wolfson JS, Hooper DC: The fluoroquinolones: structures, mechanisms of action and resistance, and spectra of activity in vitro, Antimicrobial Agents and Chemotherapy 1985; 28(4): 581-586
29. Physicians' Desk Reference. 55th ed. Montvale, Medical Economics Co, USA, 2001: 852
30. Hubicka U, Krzek J, Walczak M: Stability of ciprofloxacin and norfloxacin in the presence and absence of metal ions in acidic solution, Pharmaceutical Development and Technology 2010; 15(5): 532-44
31. Donnelly RF: Stability of Ciprofloxacin in Polyvinylchloride Minibags, The Canadian Journal of Hospital Pharmacy 2011; 64(4): 252-256.
32. Olivera ME, Manzo RH, Junginger HE, Midha KK, Shah VP, Stavchansky S, Dressman JB, Barends DM: Biowaiver Monographs for Immediate Release Solid Oral Dosage Forms : Ciprofloxacin Hydrochloride, Journal of Pharmaceutical Sciences 2011; 100(1): 22–33.
33. Zakelj S, Berginc K, Ursic D, Kristl A: Influence of metal cations on the solubility of fluoroquinolones, Die Pharmazie 2007; 62(4): 318-20
34. Slots J: Selection of antimicrobial agents in periodontal therapy, Journal of Periodontal Research 2002; 37(5): 389-98

35. Choudhury A, Das S, Dhangar S, Kapasiya S, Kanango, A: Development and Characterization Buccoadhesive Film of Ciprofloxacin Hydrochloride, International Journal of PharmTech Research 2010; 2(2): 1050–1057.
36. Soleymani Shayesteh Y, Khorsand A, Salary MH, Mehrizy H: Comparison of Systemic Ciprofloxacin in Elimination of A.a from Active Sites with Combination of Metronidzole and Amoxicillin in Patients with Aggressive Periodontitis: A Randomized Double Blind Controlled Trial, Journal of Dentistry of Tehran University of Medical Sciences 2004; 1(2): 24-28.
37. Ednie LM, Jacobs MR, Appelbaum PC: Activities of Gatifloxacin Compared to Those of Seven Other Agents against Anaerobic Organisms, Antimicrobial Agents and Chemotherapy 1998; 42(9): 2459–2462.
38. Pajukanta R, Asikainen S, Forsblom B, Saarela M, Jousimies-Somer H: β-Lactamase production and in vitro antimicrobial susceptibility of *Porphyromonas gingivalis*. FEMS Immunology & Medical Microbiology 1993, 6: 241-244
39. Jain P, Pundir RK: Antibiotic sensitivity pattern of Streptococcus mutans against commercially available drugs, Journal of Pharmacy Research 2009; 2(7): 1250-1252
40. Chowdaiah M, Dhamodhar P: Antibacterial properties of honey and green tea extracts against multi-drug resistant *Streptococcus mutans* isolated from dental plaque samples, International Journal of Pharma and Bio Sciences 2017; 8(2): 547–552.
41. Mittal S, Soni H, Sharma DK, Mittal K, Pathania V, Sharma S: Comparative evaluation of the antibacterial and physical properties of conventional glass ionomer cement containing chlorhexidine and antibiotics, Journal of International Society of Preventive & Community Dentistry 2015; 5(4): 268-275
42. Johnston D, Choonara YE, Kumar P, Du Toit LC, Van Vuuren S, Pillay V: Prolonged delivery of ciprofloxacin and diclofenac sodium from a polymeric fibre device for the treatment of peridontal disease, BioMed Research International 2013: 460936
43. Zupančič Š: Razvoj dvoslojnih nanovlaken za inovativno zdravljenje parodontalne bolezni, UNI LJ FFA, 2017; doktorska disertacija

44. Huang ZM, Zhang YZ, Kotaki M, Ramakrishna S: A review on polymer nanofibers by electrospinning and their applications in nanocomposites, Composites Science and Technology 2003; 63(15): 2223–2253
45. Patanaik A, Anandjiwala RD, Rengasamy RS, Ghosh A: Nanotechnology in fibrous materials – a new perspective, Textile progress 2007; 9(2): 67-120
46. Joshi D, Garg T, Goyal AK, Rath G: Advanced drug delivery approaches against periodontitis Advanced drug delivery approaches against periodontitis, Drug Delivery 2016; 23(2): 363-77
47. Rošic Danko R.: Tiny secrets of modern wound healing, Farmacevtski vestnik 2016; 67: 227-234
48. Abrigo M, McArthur SL, Kingshott P: Electrospun nanofibers as dressings for chronic wound care: Advances, challenges, and future prospects, Macromolecular Bioscience 2014; 14(6): 772-92
49. Pelipenko J, Kocbek P, Kristl J: Critical attributes of nanofibers: Preparation, drug loading, and tissue regeneration, International Journal of Pharmaceutics 2015; 484(1–2): 57-74
50. Širc J, Hobzova R, Kostina N, Munzarov M, Jukličkova M, Lhotka M, Kubinova Š, Zajicova A, Michalek J: Morphological Characterization of Nanofibers: Methods and Application in Practice, Journal of Nanomaterials 2012: 327369
51. Zamani M, Prabhakaran MP, Ramakrishna S: Advances in drug delivery via electrospun and electrosprayed nanomaterials, International Journal of Nanomedicine 2013; 8:2997-3017
52. Khan WS, Asmatulu R., Ceylan M, Jabbarnia A: Recent Progress on Conventional and Non- Conventional Electrospinning Processes, Fibers and Polymers 2013; 14(8): 1235-1247
53. Osathanon T, Chanjavanakul P, Kongdecha P, Clayhan P. Huynh NCN: Polycaprolactone-Based Biomaterials for Guided Tissue Regeneration Membrane, Periodontitis - A Useful Reference 2017; 8: 171-188

54. Meredith JC, Amis EJ: LCST phase separation in biodegradable polymer blends: poly(D,L -lactide) and poly(ε - caprolactone), Macromolecular Chemistry and Physics 1999; 201: 733–739
55. Labet M, Thielemans W: Synthesis of polycaprolactone : a review, Chemical Society Reviews 2009; 38(12): 3484-504
56. Langer R, Chasin M: Biodegradable polymers as drug delivery systems, Marcel Decker, USA, 1990; 70-112
57. Malathi K, Jeevarekha M, Rajula MPB, Singh A: Local Drug Delivery – A Targeted Approach, International Journal of Bioscience and Medicine. 2014; 3(2): 29-34
58. Richard WB: Controlled release drug delivery system for the periodontal pocket, United States Patent, Patent number 4,780,320, date of patent 25.10.1988
59. Rošic R, Kocbek P, Pelipenko J, Kristl J, Baumgartner S: Nanofibers and their biomedical use, Acta Pharmaceutica 2013; 63(3): 295-304
60. Zamani M, Morshed M, Varshosaz J, Jannesari M: Controlled release of metronidazole benzoate from poly ε-caprolactone electrospun nanofibers for periodontal diseases, European Journal of Pharmaceutics and Biopharmaceutics 2010; 75(2): 179–185
61. Zupančič Š, Sinha-Ray S, Sinha-Ray S, Kristl J, Yarin AL: Long-term sustained ciprofloxacin release from PMMA and hydrophilic polymer blended nanofibers, Molecular pharmaceutics, 2016; 13(1): 295-305.
62. Chaturvedi TP, Srivastava R, Srivastava AK, Gupta V, Verma PK: Doxycycline poly ε - caprolactone nanofibers in patients with chronic periodontitis- a clinical evaluation 2013; Journal of Clinical and Diagnostic Research 2013; 7(10): 2339-42
63. ISO standard 10993-5, Third edition 2009-06-01: Biological evaluation of medical devices Part 5: Tests for in vitro cytotoxicity
64. Sill TJ, Recum, HA: Electrospinning: Applications in drug delivery and tissue engineering, Biomaterials 2008; 29(13): 1989-2006
65. Bottino MC, Kamocki K, Yassen GH, Platt JA, Vail MM, Ehrlich Y, Spolnik KJ, Gregory RL: Bioactive Nanofibrous Scaffolds for Regenerative Endodontics Bioactive Nanofibrous Scaffolds for Regenerative Endodontics, Journal of Dental Research 2013; 92(11): 963-969

66. Bottino MC, Arthur RA, Waeiss RA, Kamocki K, Gregson SK, Gregory RL: Biodegradable nanofibrous drug delivery systems: Effects of metronidazole and ciprofloxacin on periodontopathogens and commensal oral bacteria, Clinical Oral Ivestigations 2014; 18(9): 2151–2158.
67. Unnithan AR, Barakat NA, Pichiah PB, Gnanasekaran G, Nirmala R, Cha YS, Jung CH, El-Newehy M, Kim HY: Wound-dressing materials with antibacterial activity from electrospun polyurethane-dextran nanofiber mats containing ciprofloxacin HCl, Carbohydrate Polymers 2012; 90(4): 1786-93
68. Baghel S, Cathcart H, Reilly NJ: Polymeric Amorphous Solid Dispersions: A Review of Amorphization, Crystallization, Stabilization, Solid-State Characterization, and Aqueous Solubilization of Biopharmaceutical Classification System Class II Drugs, Journal of Pharmaceutical Science 2016; 105(9): 2527-2544
69. Yu DG, Branford-white C, White K, Li XL, Zhu LM: Dissolution Improvement of Electrospun Nanofiber-Based Solid Dispersions for Acetaminophen, AAPS PharmSciTech. 2010; 11(2): 809-17
70. Natarajan V, Krithica N, Madhan B, Sehgal PK: Formulation and Evaluation of Quercetin Polycaprolactone Microspheres for the Treatment of Rheumatoid Arthritis, Journal of Pharmaceutical Sciences 2011; 100(1): 195–205.
71. Lam YL, Muniyandy S, Kamaruddin H, Mansor A, Janarthanan P: Radiation cross-linked carboxymethyl sago pulp hydrogels loaded with ciprofloxacin: Influence of irradiation on gel fraction, entrapped drug and in vitro release, Radiation Physics and Chemistry 2015; 106: 213-222
72. Kumar S, Parthiban S, Kumar SKS: Formulation and evaluation of meloxicam loaded for microspheres for colon targeted drug delivery, International Journal of Biopharmaceutics 2013; 4(3): 80–89.
73. Potrč T, Baumgartner S, Roškar R, Planinšek O, Lavrič Z, Kristl J, Kocbek P: Electrospun polycaprolactone nanofibers as a potential oromucosal delivery system for poorly water-soluble drugs, European Journal of Pharmaceutical Sciences 2015; 75: 101-113
74. Hubicka U, Żmudzki P, Talik P, Żuromska-Witek B, Krzek J: Photodegradation assessment of ciprofloxacin, moxifloxacin, norfloxacin and ofloxacin in the presence of

excipients from tablets by UHPLC-MS/MS and DSC, Chemistry Central Journal. 2013; 7:133

75. Sahoo S, Mishra S, Chakraborti C: Qualitative analysis of controlled release ciprofloxacin/carbopol 934 mucoadhesive suspension, Journal of Advanced Pharmaceutical Technology & Research. 2011; 2(3):195-204
76. Gonzalez FM, Cortez JI, Gonzalez Cortez MA, Moreno Rodriguez JA, Romero JS, Hernandez Apam MA, Gomez Velasco HS: Cubic Spline and Characterization of Metronidazole to Determine the Changes in the Solid Solution, International Journal of Mathematical Models and Methods in Applied Sciences 2011; 5(3): 454–462.
77. Nohemann L, Almeida MP, Ferrari PC: Floating ability and drug release evaluation of gastroretentive microparticles system containing metronidazole obtained by spray drying, Brazilian Journal of Pharmaceutical Sciences 2015; 53(1): 1–13
78. Meng ZX, Zheng W, Li L, Zheng YF: Fabrication and characterization of three-dimensional nano fi ber membrance of PCL – MWCNTs by electrospinning, Materials Science and Engineering 2010; 30(7): 1014-1021
79. Demirci S, Celebioglu A, Aytac Z, Uyar T: pH-responsive nanofibers with controlled drug release properties. Polymer Chemistry 2014; 5(6): 2050–2056.
80. Ignatova M, Rashkov I, Manolova N: Drug-loaded electrospun materials in wound-dressing applications and in local cancer treatment, Expert Opinion on Drug Delivery 2013; 10(4): 469-483
81. El-Newehy MH, Al-deyab SS, Kenawy ER, Abdel-Megeed A: Fabrication of Electrospun Antimicrobial Nanofibers Containing Metronidazole Using Nanospider Technology, Fibers and Polymers 2012; 13(6): 709-717
82. Trivedi MK, Patil S, Shettigar H, Bairwa K, Jana S: Spectroscopic Characterization of Biofield Treated Metronidazole and Tinidazole, Medicinal Chemistry 2015; 5(7): 340–344.
83. Megalai SM, Manjula P, Manonmani KN, Kavitha N, Baby N: Metronidazole: A Corrosion Inhibitor for Mild Steel in Aqueous Environment, Portugaliae Electrochimica Acta 2012, 30(6), 395–403.

84. Patel YL, Sher P, Pawar AP: The effect of drug concentration and curing time on processing and properties of calcium alginate beads containing metronidazole by response surface methodology, AAPS PharmSciTech 2006; 7(4): 1–7.
85. De Giglio E, Bonifacio MA, Cometa S, Vona D, Mattioli-Belmonte M, Dicarlo M, Ceci E, Fino V, Cicco SR, Farinola GM: Data on glycerol/tartaric acid-based copolymer containing ciprofloxacin for wound healing applications, Data in Brief. 2016; 11(7): 1335-40
86. Patel KS, Patel JS, Dholariya HR, Patel VK, Patel KD: Synthesis of Cu (II), Ni (II), Co (II), and Mn (II) Complexes with Ciprofloxacin and Their Evaluation of Antimicrobial , Antioxidant and Anti-Tubercular Activity, Open Journal of Metal 2012; 2(3): 49-59
87. Silva-Junior AA, Scarpa MV, Pestana KC, Mercuri LP, Rosario de Matos J, Gomes de Oliveira A: Thermal analysis of biodegradable microparticles containing ciprofloxacin hydrochloride obtained by spray drying technique, Thermochimica Acta 467, 2008; 91–98
88. Shi P, Zuo Y, Zou Q, Shen J, Zhang L, Li Y, Morsi YS: Improved properties of incorporated chitosan film with ethyl cellulose microspheres for controlled release, International Journal of Pharmaceutics 2009; 375(1–2): 67–74
89. Hoidy WH, Ahmad MB, Jaffar Al-Mulla EA, Azowa Bt Ibrahim N: Preparation and Characterization of Polylactic Acid/Polycaprolactone Clay Nanocomposites, Journal of Applied Sciences 2010; 10(2): 97-106
90. Singh S, Wu BM, Dunn JCY: The enhancement of VEGF-mediated angiogenesis by polycaprolactone scaffolds with surface cross-linked heparin, Biomaterials 2011; 32(8): 2059–2069
91. Chakrapani VY, Gnanamani A, Giridev VR, Madhusoothanan M, Sekaran G: Electrospinning of type I collagen and PCL nanofibers using acetic acid, Journal of Applied Polymer Science 2012; 125: 3221–3227.
92. Shalumon, KT, sowmya S, Sathish D, Chennazhi KP, Nair SV, Jayakumar R: Effect of Incorporation of Nanoscale Bioactive Glass and Hydroxyapatite in PCL/Chitosan Nanofibers for Bone and Periodontal Tissue Engineering, Journal of Biomedical Nanotechnology 2013; 9(3): 430-440

93. Oliveira JE, Mattoso LHC, Orts WJ, Medeiros ES: Structural and Morphological Characterization of Micro and Nanofibers Produced by Electrospinning and Solution Blow Spinning: A Comparative Study, Advances in Materials Science and Engineering 2013; 409572: 1-14
94. Cui W, Zhou Y, Chang J: Electrospun nanofibrous materials for tissue engineering and drug delivery, Science and Technology of Advanced Materials2010; 11(1): 1-11
95. Ruszczak Z, Friess W: Collagen as a carrier for on-site delivery of antibacterial drugs 2003; Advanced Drug Delivery Reviews 2003; 55(12): 1679-1698
96. Feng K, Sun H, Bradley MA, Dupler EJ, Giannobile WV, Ma PX: Novel Antibacterial Nanofibrous PLLA scaffolds, Journal of controlled release 2010; 146(3): 363–369
97. Petelin M, Zupančič Š, Baumgartner S, Lavrič Z, Kristč J: Local delivery of resveratrol using polycaprolactone nanofibers for treatment of periodontal disease, Journal of Drug Delivery Science and Technology 30 2015; 408-416
98. Hu X, Liu S, Zhou G, Huang Y, Xie Z, Jing X: Electrospinning of polymeric nanofibers for drug delivery applications, Journal of Controlled Release 2014; 185: 12–21.
99. Bickel M, Munoz JL, Giovannini P: Acid-Base Properties of Human Gingival Crevicular Fluid, Journal of Dental Research 1985; 64(10): 1–4.
100. Dang NTT, Turner MS, Coombes AGA: Development of intra-vaginal matrices from polycaprolactone for sustained release of antimicrobial agents, Journal of Biomaterials Applications 2012; 28(1):74 - 83
101. Puga AM, Rey-Rico A, Magarin Os B, Alvarez-Lorenzo C, Concheiro A: Hot melt poly-ε-caprolactone/poloxamine implantable matrices for sustained delivery of ciprofloxacin. Acta Biomaterialia. 2012; 8: 1507-1518.
102. Majdi A, Aminifard S, Zafari M, Aj J, Biazar E, Jafarpour M, Montazeri M, Akbari HR, Rad HG: Nanotoxicology and nanoparticle safety in biomedical designs, International Journal of Biomedicine 2011; 6: 1117–1127.
103. Flores-Cedillo ML, Alvarado-Estrada KN, Pozos-Guillén AJ, Murguía-Ibarra JS, Vidal MA, Cervantes-Uc JM, Rosales-Ibáñez R, Cauich-Rodríguez JV: Multiwall carbon nanotubes / polycaprolactone scaffolds seeded with human dental pulp stem cells for bone tissue regeneration, Journal of Materials Science: Materials in Medicine 2016; 27(2): 35

104. Merrell JG, McLaughlin SW, Tie L, Laurencin CT, Chen AF, Nair LS: Curcumin Loaded Poly(ε-Caprolactone) Nanofibers: Diabetic Wound Dressing with Antioxidant and Anti-inflammatory Properties, Clinical and experimental pharmacology & physiology 2009; 36(12): 1149-1156
105. Alexandrescu L, Syverud K, Gatti A, Chinga-Carrasco G: Cytotoxicity tests of cellulose nanofibril-based structures, Cellulose 2013; 20(4): 1765-1775
106. Powers KW, Palazuelos M, Moudgil BM, Roberts SM: Characterization of the size, shape, and state of dispersion of nanoparticles for toxicological studies, Nanotoxicology 2009; 1(1): 42-51
107. Müller HD, Cvikl BB, Lussi AA, Gruber RR: Salivary pellets induce a pro-inflammatory response involving the TLR4 – NF-kB pathway in gingival fibroblasts, BMC Oral Health 2016; 17(1): 15
108. Kaplan JA, Liu R, Freedman JD, Padera R, Schwartz J, Colson YL, Grinstaff MW: Prevention of lung cancer recurrence using cisplatin-loaded superhydrophobic nanofiber meshes, Biomaterials 2016; 76: 273-281
109. Changotade S, Bostan GR, Consalus A, Poirier F, Peltzer J, Lataillade JJ, Rohman G, Lutomski D: Preliminary In Vitro Assessment of Stem Cell Compatibility with Cross-Linked Poly (ε-caprolactone urethane) Scaffolds Designed through High Internal Phase Emulsions, Stem Cells International 2015;1-8
110. Hassan MI, Sun T, Sultana N: Fabrication of Nanohydroxyapatite / Poly (ε-caprolactone) Composite Microfibers Using Electrospinning Technique for Tissue Engineering Applications, Journal of Nanomaterials 2014; 65:1-7
111. Tariq M, Yasmin S, Hafeez FY: Biological Control Of Potato Black Scurf By Rhizosphere Associated Bacteria, Brazilian Journal of Microbiology 2010; 41:439-451
112. Reise M, Wyrwa R, Müller U, Zylinski M, Völpel A, Schnabelrauch M, Berg A, Jandt KD, Watts DC, Sigusch BW: Release of metronidazole from electrospun poly(l-lactide-co-d/l - lactide) fibers for local periodontitis treatment, Dental Materials 2012; 28(2): 179–188.

113. Takushige T, Cruz EV, Moral AA, Hoshino E: Endodontic treatment of primary teeth using a combination of antibacterial drugs, International Endodontic Journal 2004; 37(2): 132-138
114. Sato I, Kota K, Iwaku M, Hoshino E, Ando-Kurihara N: Sterilization of infected root-canal dentine by topical application of a mixture of ciprofloxacin, metronidazole and minocycline in situ, International Endodontic Journal. 1996; 29(2): 118-124
115. Windley W, Teixeira F, Levin L, Sigurdsson A, Trope M: Disinfection of Immature Teeth with a Triple Antibiotic Paste, International Endodontic Journal 2005; 31(6): 439-443

7 SUPPLEMENT

Table I: Results of cytotoxicity of nanofibers on BHK fibroblasts (MTZ-nanofibers with metronidazole, CPR-nanofibers with ciprofloxacin, CM-nanofibers with both drugs, PCL-nanofibers without drug).

DIRECT METHOD				
	TOTAL NUMBER OF CELLS (10^5/mL)	LIVE CELLS (10^5/mL)	DEAD CELLS	VIABILITY (%)
MTZ1	3,5	2,8	7,0x10^4	81
MTZ2	5,4	4,4	1,1x10^5	81
MTZ3	5,6	4,2	1,4x10^5	75
CPR1	1,9	1,3	6,4x10^4	68
CPR2	1,5	1	5,0x10^4	67
CPR3	3	1,9	1,1x10^5	63
combination1	3,4	3	4,0x10^4	88
CM2	3,9	3,4	5,0x10^4	87
CM3	1,8	1,3	5,0x10^4	72
PCL1	4,6	3,5	1,1x10^5	77
PCL2	3,9	3,1	9,0x10^4	78
PCL3	2,9	2,1	8,0x10^4	72
media 1	3,6	2,5	1,1x10^5	69
media 2	3,3	2,7	6,0x10^4	83
			average	**75,78571**
			st.dev.	**7,667901**
INDIRECT METHOD				
	TOTAL NUMBER OF CELLS (10^5/mL)	LIVE CELLS (10^5/mL)	DEAD CELLS	VIABILITY (%)
MTZ1	3,7	2,4	1,3x10^5	65
MTZ2	6,8	5,3	1,5x10^5	78
MTZ3	4,5	3,8	7,0x10^4	85
MTZ4	3,6	2,3	1,3x10^5	65
CPR1	5,8	4,5	1,3x10^5	78
CPR2	4,7	3,9	8,4x10^4	84
CPR3	4,2	3,2	1,0x10^5	76
CM1	3,4	2,9	5,0x10^4	85
CM2	3,7	3	7,0x10^4	82
CM3	3,3	2,7	7,0x10^4	80
PCL1	3,3	2,8	5,0x10^4	85
PCL2	4,8	2,9	1,1x10^5	73
PCL3	2,8	1,8	1,1x10^5	63
PCL4	5,3	3,3	2,0x10^5	62
media 1	5,5	4,3	1,2x10^5	78
media 2	2,7	1,9	8,0x10^4	70
			average	**75,5625**
			st. dev.	**8,245959**
Tritone X	below detection	below detection	2,0x10^4	40